NREL/TP-425-8196 • UC Category: 1504 • DE95009277

Elimination of Abnormal Combustion in a Hydrogen-Fueled Engine

M. R. Swain
M. N. Swain
University of Miami
Coral Gables, Florida
Analytical Technologies, Inc.
Miami, Florida

National Renewable Energy Laboratory
1617 Cole Boulevard
Golden, Colorado 80401-3393
A national laboratory of the U.S. Department of Energy
Managed by the Midwest Research Institute
for the U.S. Department of Energy
Under Contract No. DE-AC36-83CH10093

Prepared under Subcontract No. XS-2-12130-1

November 1995

NOTICE

Available to DOE and DOE contractors from:
Office of Scientific and Technical Information (OSTI)
P.O. Box 62
Oak Ridge, TN 37831
Prices available by calling (615) 576-8401

Available to the public from:
National Technical Information Service (NTIS)
U.S. Department of Commerce
5285 Port Royal Road
Springfield, VA 22161
(703) 487-4650

Elimination of Abnormal Combustion in a Hydrogen-Fueled Engine

Michael R. Swain
University of Miami
Coral Gables, FL

Matthew N. Swain
Analytical Technologies, Inc.
Miami, FL

ABSTRACT

The following report covers the design, construction, and testing of a dedicated hydrogen-fueled engine. Both part-load and full-load data were taken under laboratory conditions. The engine design included a billet aluminum single combustion chamber cylinder-head with one intake valve, two sodium cooled exhaust valves, and two spark plugs. The cylinder-head design also included drilled cooling passages. The fuel-delivery system employed two modified Siemens electrically actuated fuel injectors. The exhaust system included two separate headers, one for each exhaust port. The piston/ring combination was designed specifically for hydrogen operation.

INTRODUCTION

This report describes the design, construction, testing, and data obtained from a dedicated hydrogen-fueled engine. The dedicated hydrogen-fueled engine is the descendant of a gasoline-fueled engine that was converted to hydrogen-fueled operation in previous work utilizing the original gasoline cylinder head design. The purpose of this project was to determine if redesigning the engine would eliminate the high load knock and pre-ignition recorded with modified gasoline engines. The dedicated hydrogen-fueled engine required the manufacture of an extensively redesigned cylinder-head.

The design process for the dedicated hydrogen-fueled engine was broken into two parts

1. Specification of design constraints
2. Incorporation of design constraints

The design/construction process used commercially available engine parts, where possible, and the machining of components from raw materials where necessary.

The testing process section describes the testing apparatus and procedures used.

The data section presents the raw data, the performance maps describing engine performance, and the methods used to generate them.

DESIGN PROCESS

The design constraints influencing engine design were as follows

1. Because previous work had shown inherently high energy release rates in stoichiometric hydrogen-air mixtures, a low-turbulence combustion chamber was desirable to allow stoichiometric operation. A low-turbulence chamber should be designed without swirl, tumble, or squish. A disk combustion chamber, in conjunction with an axially aligned symmetric intake port, satisfies these design constraints.

2. The desire to reduce energy release rate at high equivalence ratios (stoichiometric) also mandated positioning at least one spark plug on the periphery of the disk combustion chamber.

3. Because previous work had shown inherently low energy-release rates in lean hydrogen-air mixtures, it was necessary to provide a means to increase the energy-release rate during lean operation. A second spark plug was included in the design that could be fired simultaneously with the first to initiate two flame fronts, effectively increasing the energy release rate.

4. The spark plugs were chosen to operate with low surface temperatures to prevent the development of a surface ignition site in the combustion chamber. Low surface temperatures are desirable to prevent pre-ignition of the hydrogen-air mixture, particularly

as deposits collect on the surfaces. Champion 10 mm (G55R) spark plugs (Photo 1) were chosen to meet the low temperature constraint and were of small diameter, which made them easier to include in the cylinder head design.

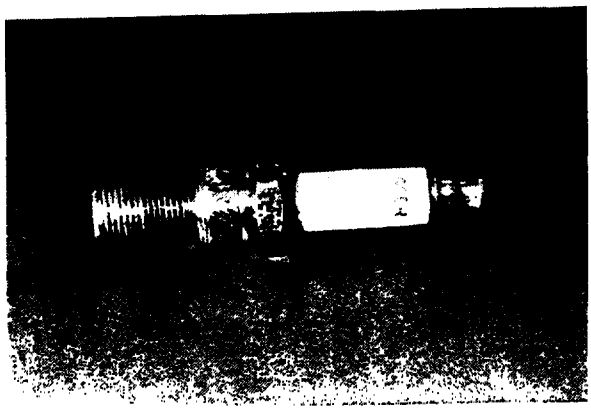

Photo 1 - Champion 10 mm (G55R) spark plug

5. The exhaust valves were also chosen to operate with low surface temperatures to prevent the development of a surface ignition site in the combustion chamber. Smaller diameter exhaust valves are easier to cool because the heat into the valve increases in proportion to the valve head area (square of valve diameter), but the heat out of the valve increases in proportion to the valve seat area (linear with valve diameter). Therefore, two small exhaust valves were used rather than one larger exhaust valve. The exhaust valves were made from Alfa Romeo 1300 cc, 9 mm stem, sodium-cooled exhaust valves. The valve head diameter was cut down to 1.0 in. The exhaust valve from the Alfa Romeo 1600 cc engine could have been used, but the sodium chamber inside the valve head was larger in the valve from the 1300 cc engine, affording better cooling.

6. To prevent ignition of the fresh charge by residuals from the previous cycle, only air was allowed to enter the cylinder during the early part of the intake stroke. This reduced the chance of early ignition in two ways. First, it reduced the amount of hydrogen that was trapped with air in the piston ring land during compression. This reduced the likelihood that combustion in the gases and oil vapor trapped in the ring land would continue into the next cycle. Second, the air dropped the temperature of the residuals before hydrogen entered the cylinder. The intake geometry and fuel injector timing was chosen to deliver an initial mixture of air with little or no hydrogen for the first 7.5 in^2 of mixture inducted. The system was designed to be insensitive to injector leakage.

7. The compression ring gaps were chosen to vent high-pressure gases accumulated between the first and second compression rings preferentially to the crank case.

8. The cooling system was designed to provide uniform coolant flow rates. The principal obstacle to heat transfer in an aluminum cylinder head is at the aluminum-coolant interface at locations where there are low flow rates of coolant and film boiling can occur. Coolant systems that avoid nonuniformities in local coolant flow rate prevent film boiling. Such a design was ideally suited to the use of the sodium-cooled exhaust valves chosen for the design of this dedicated hydrogen-fueled engine. A minimum of 0.40 inch spacing between combustion chamber components (valves, plugs) was used to provide adequate cooling.

Combustion Chamber Design

The eight previously described design constraints were incorporated into a combustion chamber to cover the 3.35 inch diameter cylinder bore (Figures 1-4). The standard lifter location and orientation for the 2TC Toyota engine were retained although it was necessary to modify the intake lifter for pushrod clearance. The combustion chamber layout shown was strongly influenced by the need to actuate the two exhaust valves with one pushrod. As can be seen in Figures 5-6, the intake port was symmetric about a vertical plane passing through the central axis of the combustion chamber. This configuration was expected to produce no swirl, but minor changes in the port during flow bench work resulted in swirl. The intake-valve-head diameter was 1.42 inches. The intake port was a slightly scaled-down duplicate of the standard Toyota 2TC intake port. The final design of the cylinder head employed very short (2 inch) exhaust ports internal to the cylinder head. This reduced the heat load to the cylinder head. A large portion of the heat load to the cylinder head and water jacket occurs in the exhaust port, so the ports were kept as short as possible.

Radial heat transfer out of the combustion chamber was absorbed by a coaxial water passage around the periphery of the combustion chamber. The passage was split into two parts, each fed by water from the cylinder block. Cooling water entered each part at the rear of the cylinder head and again at locations along their pathway, eventually exiting at the front of the cylinder head through two 0.25 inch ID fittings.

Axial heat transfer out of the top of the combustion chamber was absorbed by two 0.25 inch diameter coolant passages that entered at the rear and driver side of the engine and exited at the front of the cylinder head. The coolant was once-through city water. Coolant flow was regulated to achieve an exhaust valve seat temperature of 225 °F.

The final combustion chamber had 4.8% less surface area than the original Toyota 2TC hemispherical combustion chamber (Photo 2).

The final engine design satisfies all of the principal design criteria and almost all of the secondary design criteria. Secondary criteria 3 was not fully satisfied because spark plug 2 was not vertical. Spark plug 2 was angled 13° radially outward from the vertical, which was necessary for clearance. The G55R Champion spark plug was machined to be flush with the inside of the chamber when installed. Secondary criteria 5 was not fully satisfied because it was necessary to reduce the clearance between the valves and the combustion chamber wall to 0.01 inches. Flow bench work showed that the reduction in flow due to shrouding can be offset by improving the flow coefficient of the ports leading to the valves.

The final design is shown in Figures 1-4. The spark plugs are shown as extended cylinders to indicate the space needed for installation and removal.

The intake valve location was mandated by the location of the intake pushrod and the dimensions of the available existing rockers. A survey of existing automotive rocker arms was conducted and the rocker for a 1972, 1600 cc "Kent" 4-cylinder Ford engine was chosen. That rocker had the shortest distance between valve stem and pushrod available (2 inches). The rocker ratio was

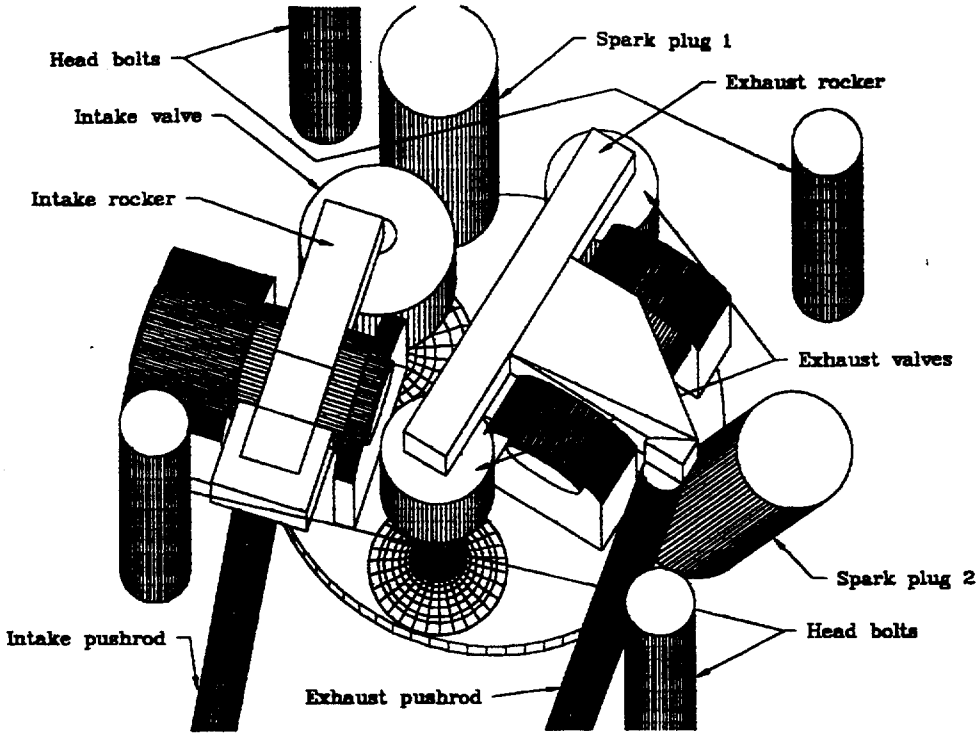

Figure 1 - CAD drawing of cylinder head

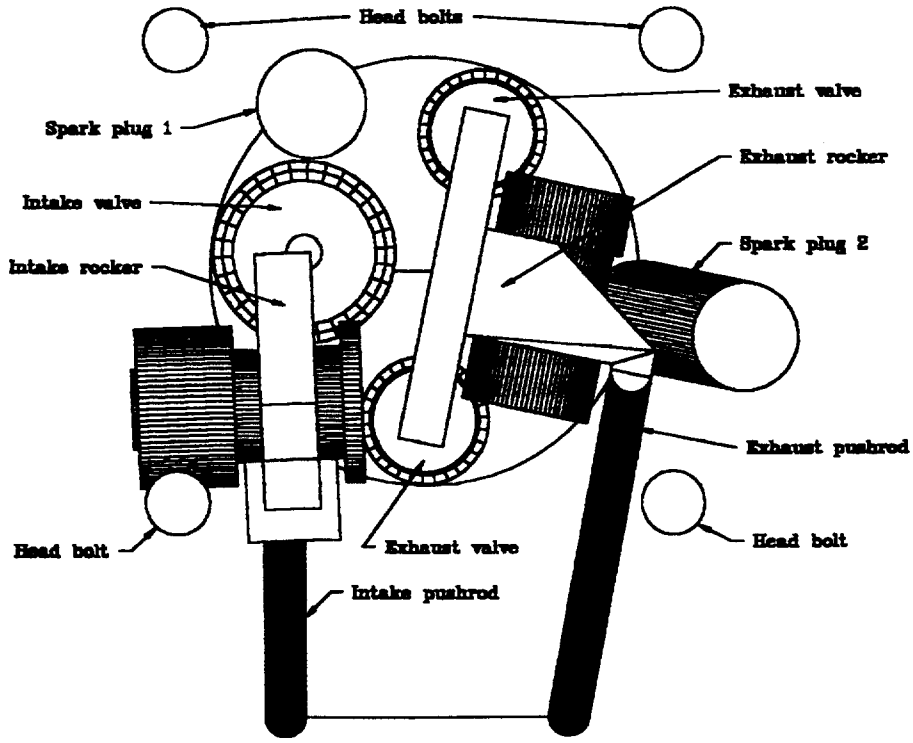

Figure 2 - CAD top view of cylinder head

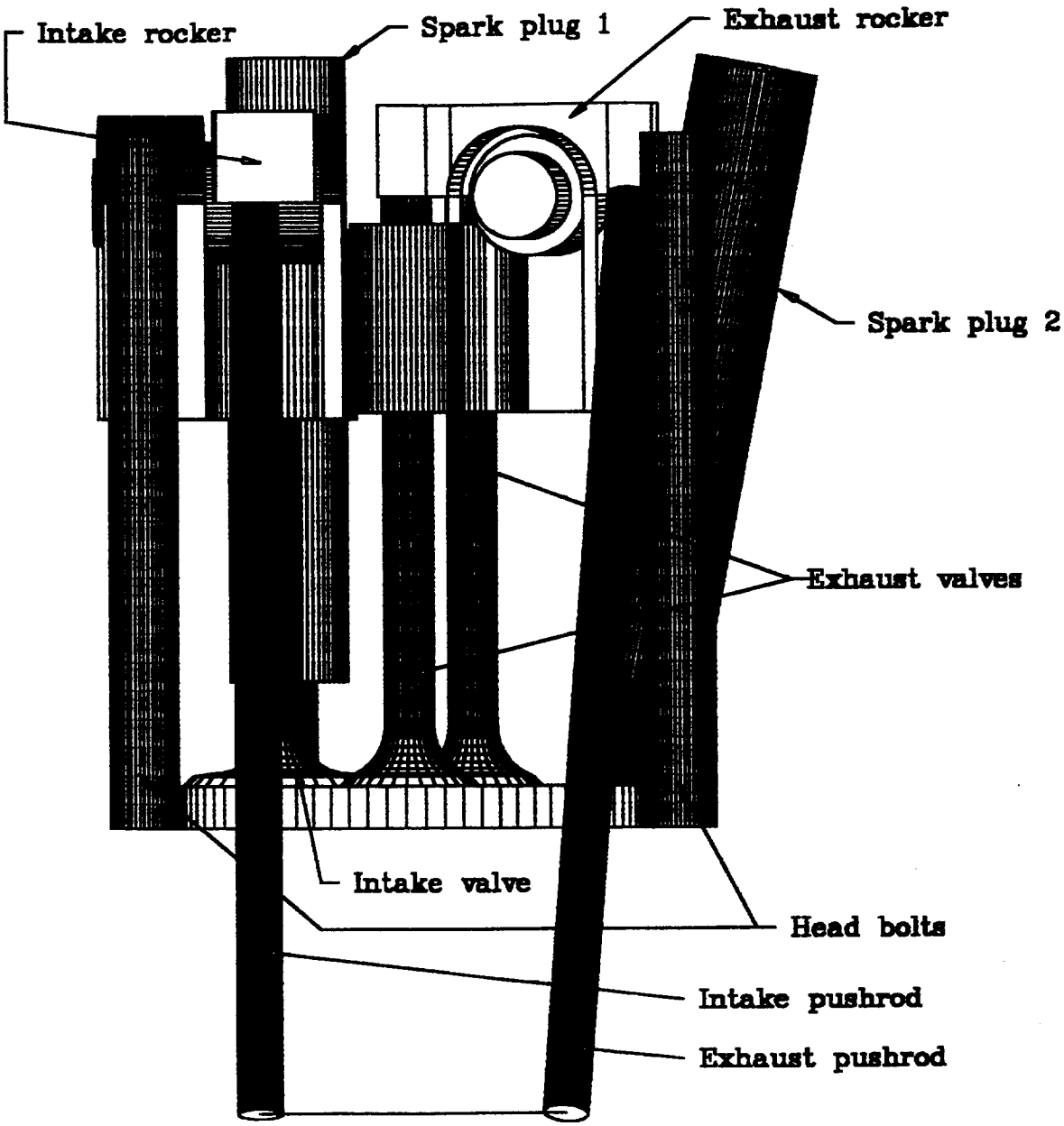

Figure 3 - CAD side view of cylinder head

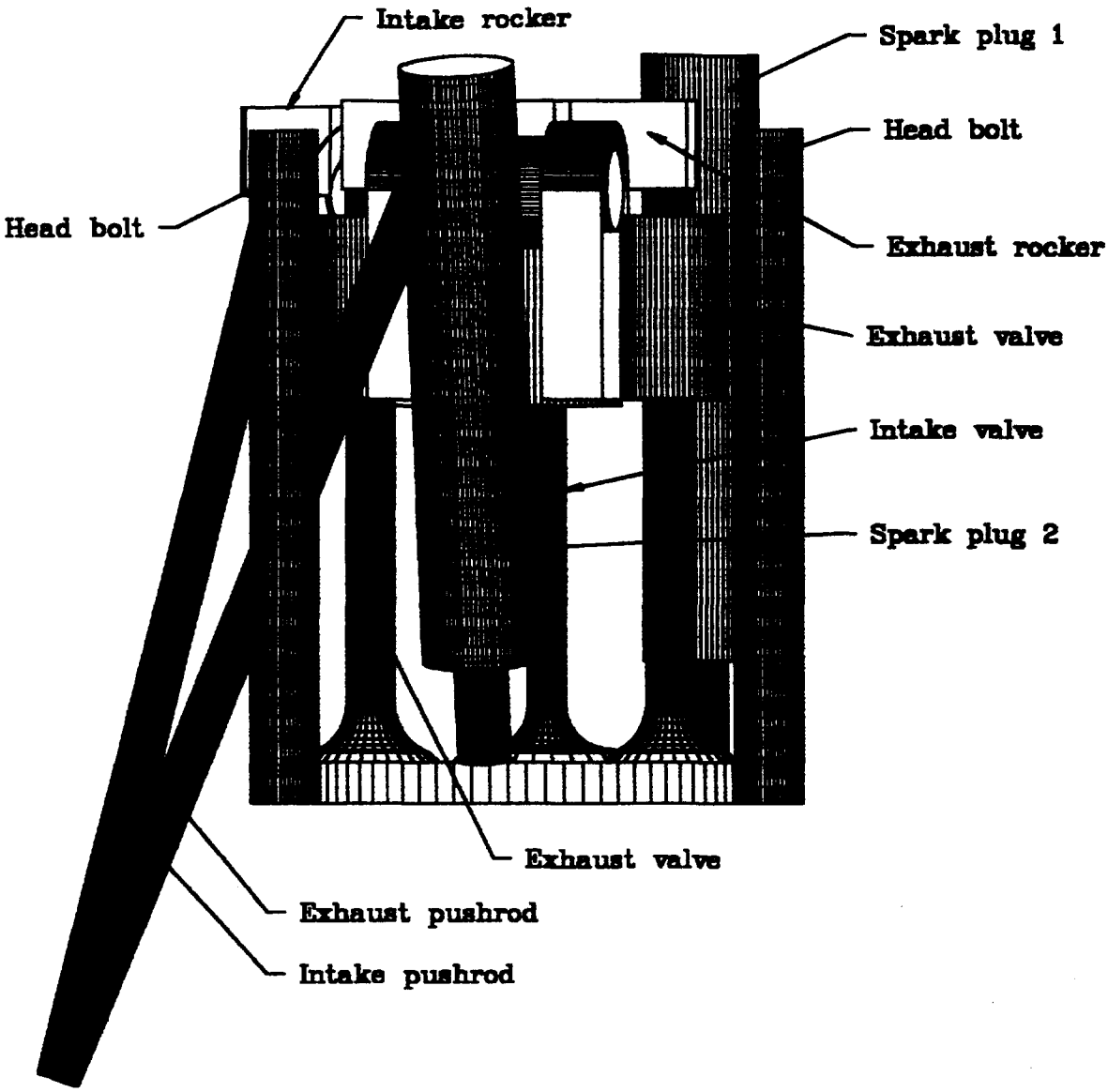

Figure 4 - CAD front view of head

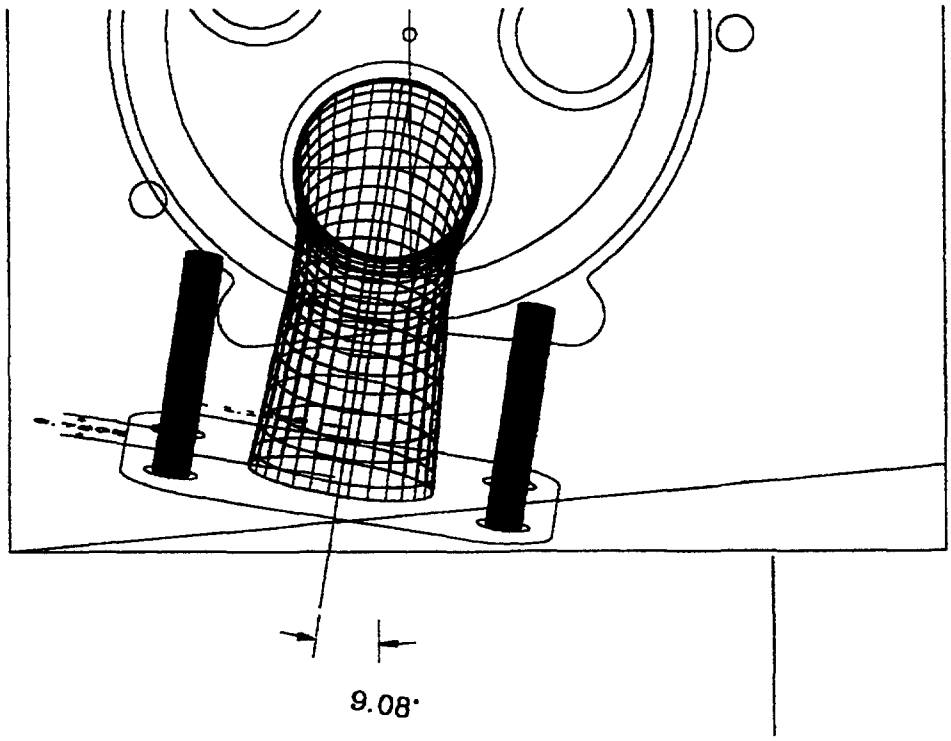

Figure 5 - CAD top view of intake port

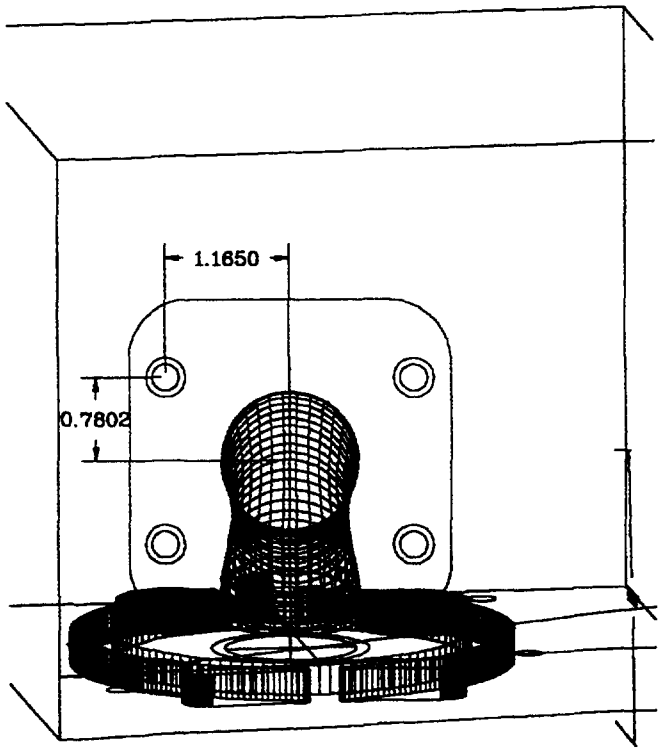

Figure 6 - CAD view directly into intake port

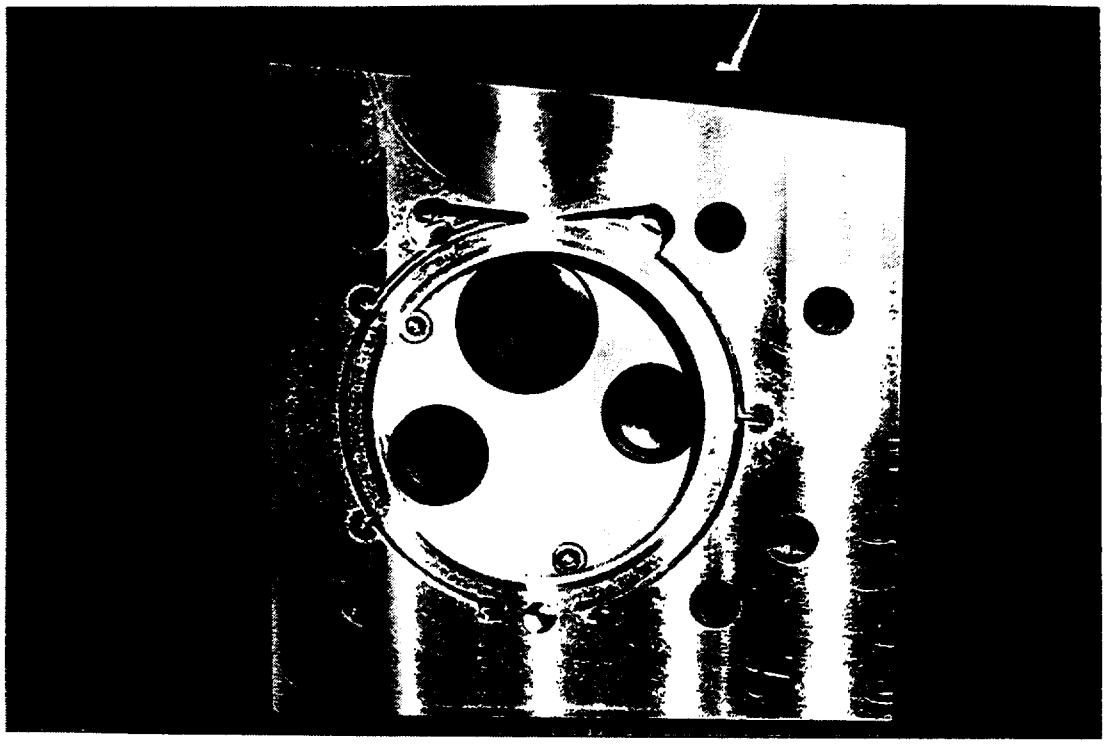

Photo 2 - Final combustion chamber after high load operation

1.455:1. The rocker ratio specifies the ratio of valve motion to pushrod motion. It was possible to use that rocker by rotating the intake pushrod 8° outward, away from the cylinder bore (pushrod can be rotated 9° maximum). This allows for an acceptable intake valve position and also allows the intake rocker to remain clear of the exhaust valves, while leaving enough room for the exhaust rocker and two spark plugs.

The two exhaust valves are actuated by the standard exhaust pushrod rotated 4° to the right as viewed in Figure 3. The rotation was limited by the head bolt position. This yielded a valve stem to pushrod length of 1.5 inches for the exhaust rocker (machined specifically for the engine). The exhaust rocker ratio was 1.0:1.

Table 1 depicts the basic dimensions of the engine.

Table 1 - Basic Dimensions
of Hydrogen-Fueled Engine

Displacement	24.6 in^3	402.0 cc
Bore	3.37 in	85.5 mm
Stroke	2.76 in	70.0 mm
Compression ratio	9.2:1	
Intake valve dia.	1.42 in	36.0 mm
Exhaust valve dia.	(2) 1.00 in	(2) 25.4 mm
Intake lift	0.329 in	8.4 mm
Exhaust lift	0.226 in	5.7 mm

Ring Gap Selection

Ring end gaps were chosen at:

0.006 in. for the top compression ring
0.010 in. for the second compression ring
0.012 in. for the top oil control ring
0.010 in. for the bottom oil control ring

These gaps were previously found to be compatible with the use of hydrogen. The tight ring gap in the top compression ring directs the leakage of high pressure gases trapped between the rings towards the crankcase instead of into the combustion chamber. These gases carry residuals and oil from the previous cycle.

Determination of Valve Timing and Exhaust System Design

The design goals for the exhaust system and valve timing were to improve volumetric efficiency over that of the Toyota 2TC engine and to reduce the amount of exhaust residuals trapped in the cylinder at the beginning of the intake stroke. The principal valve event affecting volumetric efficiency is intake valve closing. Both the literature and previous data taken with the Toyota 2TC engine provided volumetric efficiency versus revolutions per minute (RPM) curves for the engine. Based on this information, intake valve closing was chosen at 42° after bottom dead center (ABDC). The two 0.779 inch ID header pipes, one from each exhaust port, were either 5 or 6 ft. long. The finished design resulted in improvements in volumetric efficiency up to 3700 RPM. The flow field produced in the combustion chamber is shown in Photograph 3 of the combustion chamber in which oil that passed the intake valve stem seal can be seen flowing out of the exhaust port. This photo shows the "Kent" intake valve and seal that were eventually changed to the modified 1.6L Toyota 2TC valve and 2.0L Chevrolet valve stem seal because of excessive amounts of oil passing the stem seal.

The chosen cam specifications were as follows:

Intake valve opening	(IVO)	18°	before top dead center	(BTDC)
Intake valve closing	(IVC)	42°	after bottom dead center	(ABDC)
Exhaust valve opening	(EVO)	61°	before bottom dead center	(BBDC)
Exhaust valve closing	(EVC)	9°	after top dead center	(ATDC)
Intake lift	0.329 inches			
Exhaust lift	0.226 inches			

Induction System Design

The principal design criteria affecting the induction system design were the ability to deliver a relatively homogeneous mixture at light-load conditions and the ability to deliver an initial portion of pure air followed by hydrogen-air mixture at high-load conditions. The induction system was also designed to minimize intake charge heating. Figure 7 and Photos 4-7 show the final form of the engine, including the induction system. The induction system uses two

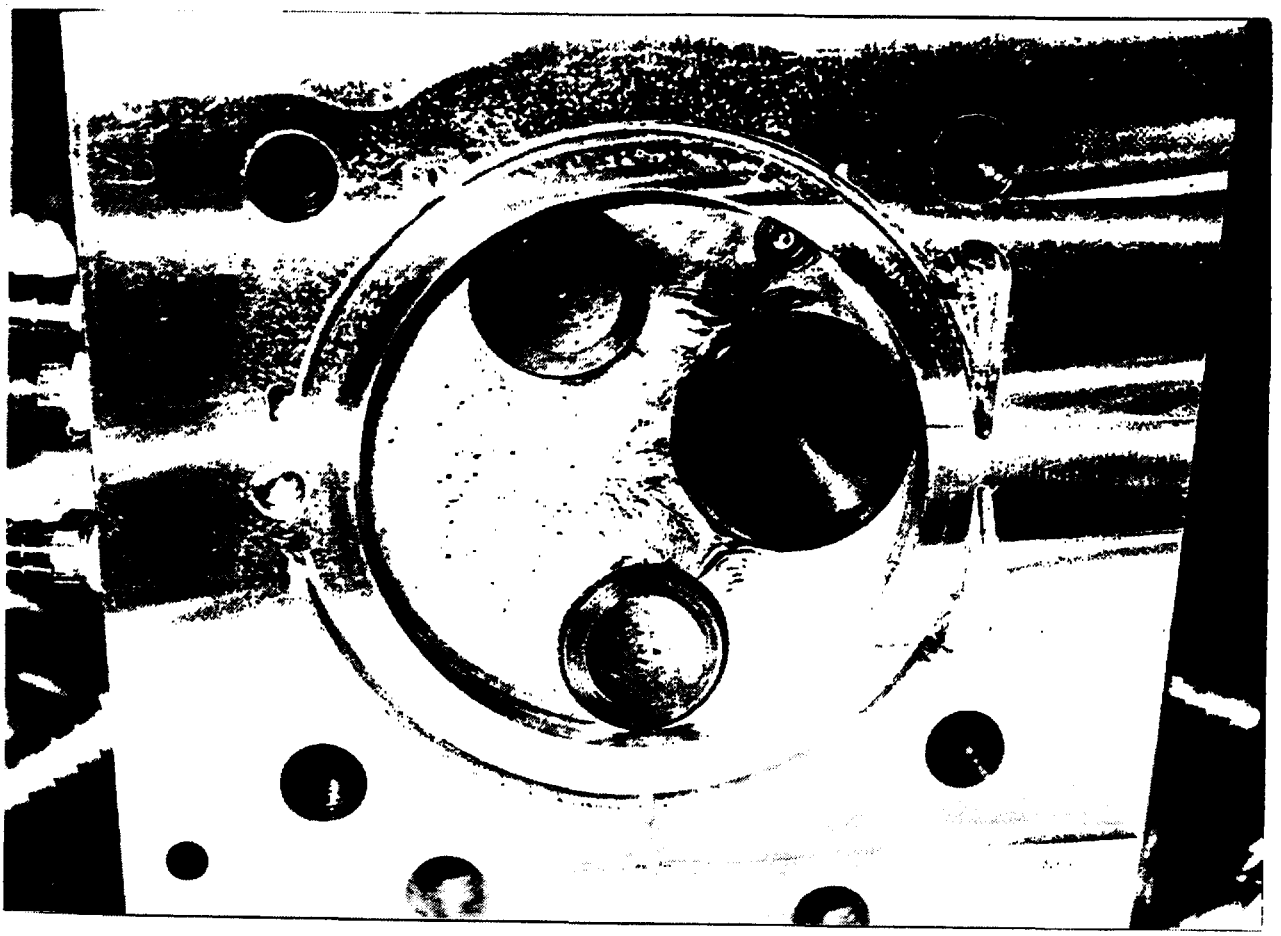

Photo 3 - Early combustion chamber configuration with oil leakage past intake valve guide

electrically actuated high-flow rate fuel injectors (Photo 8) supplied by Siemens Automotive. The injectors were tested at up to 60 psig to measure leakage. Leakage was measured by connecting the injector to a bubble meter. The leakage rate was computed by measuring the travel time of the bubble in the calibrated bubble meter tube with a stop watch. At 60 psi, the leakage rate was 2.48 ml/sec and 2.14 ml/sec. The maximum hydrogen delivery pressure was 45 psig, so the sealing ability was more than adequate. Injection duration was controlled with an Intelligent Controls IC5130 fuel-injector controller. A hall sensor with a magnet mounted on the camshaft (Photo 9) triggered the control unit at 21° BTDC.

The injection timing for each data point is given in Appendix A. The duration of injection was limited to prevent injection after 90° ATDC. The injector required 0.7 ms to close. This allowed the intake manifold to be filled with air as the final mixture was drawn into the cylinder. The intake manifold then remained filled with air until the next intake stroke.

The two injectors deliver fuel at the minor diameter of the throttle body. They were aimed parallel to, but offset 0.15 inches from, a radial line drawn from the central axis of the venturi. The intake manifold was 4 inches long and was constructed from 0.049 inch wall 1.5 inch OD aluminum tubing. 7.5 inches of clear plastic tubing of 0.20 inch wall thickness was installed to insulate the inside of the throttle body, intake manifold, and the first 1.75 inches of the intake

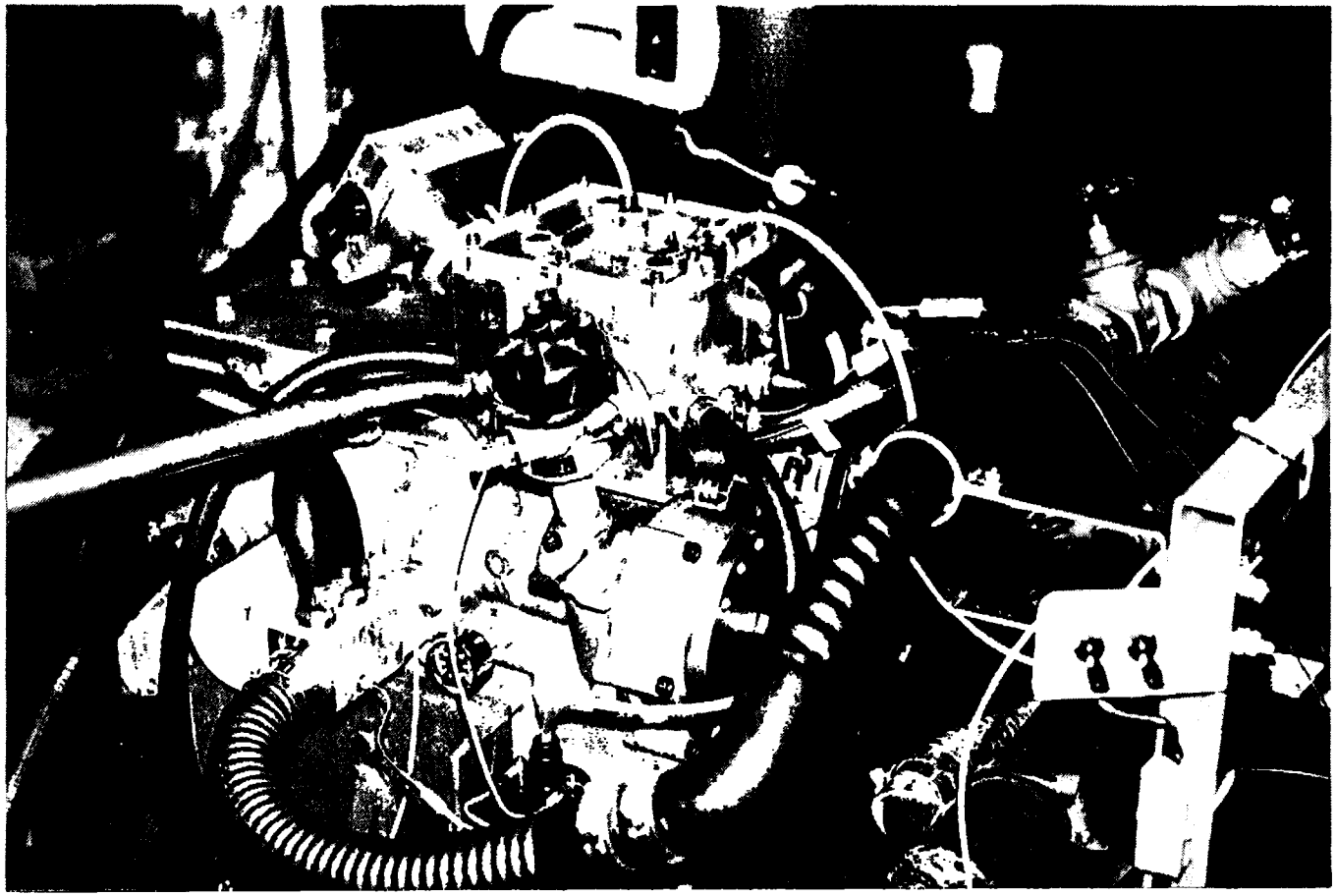

Photo 4 - Fully assembled engine

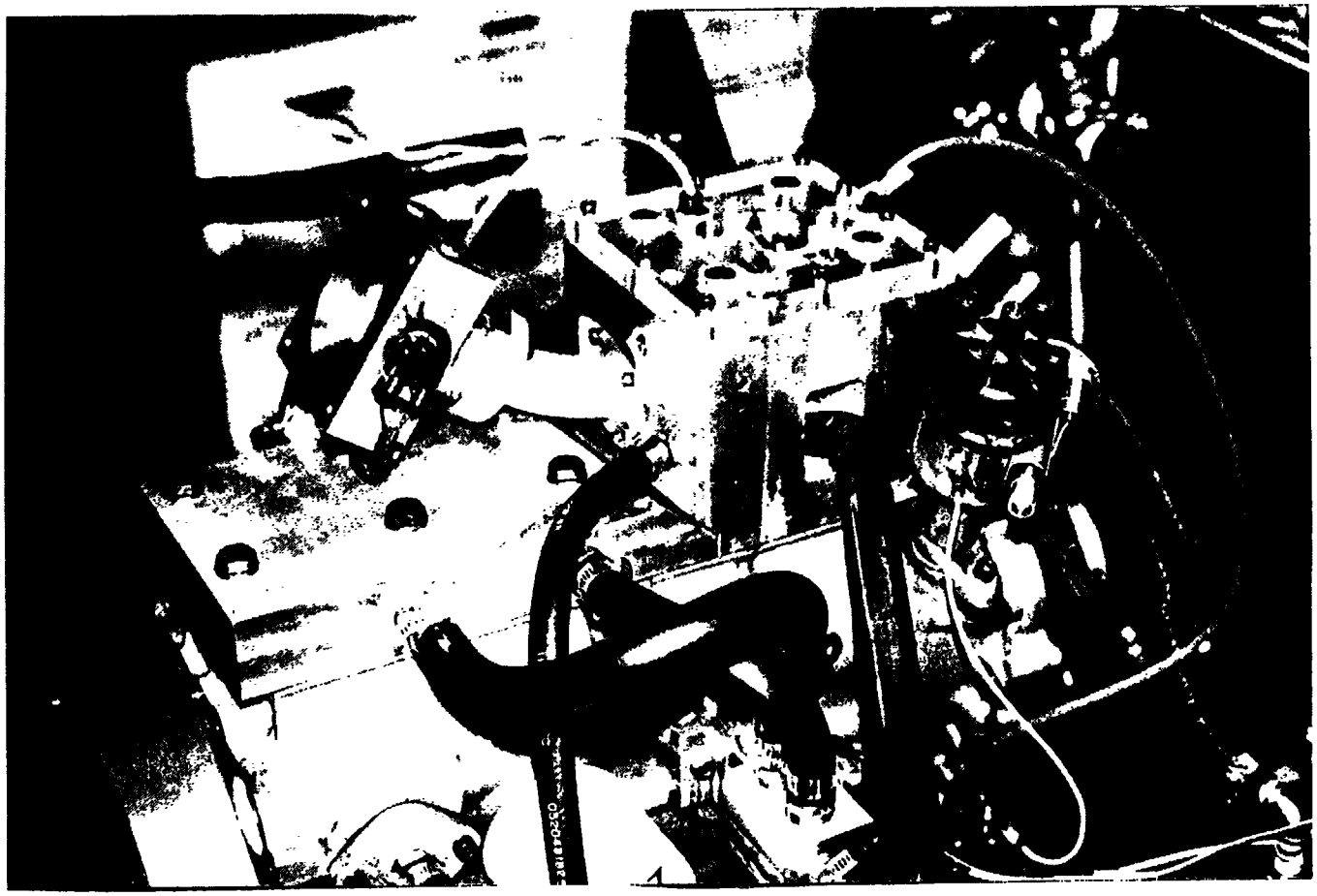

Photo 5 - Fully assembled engine

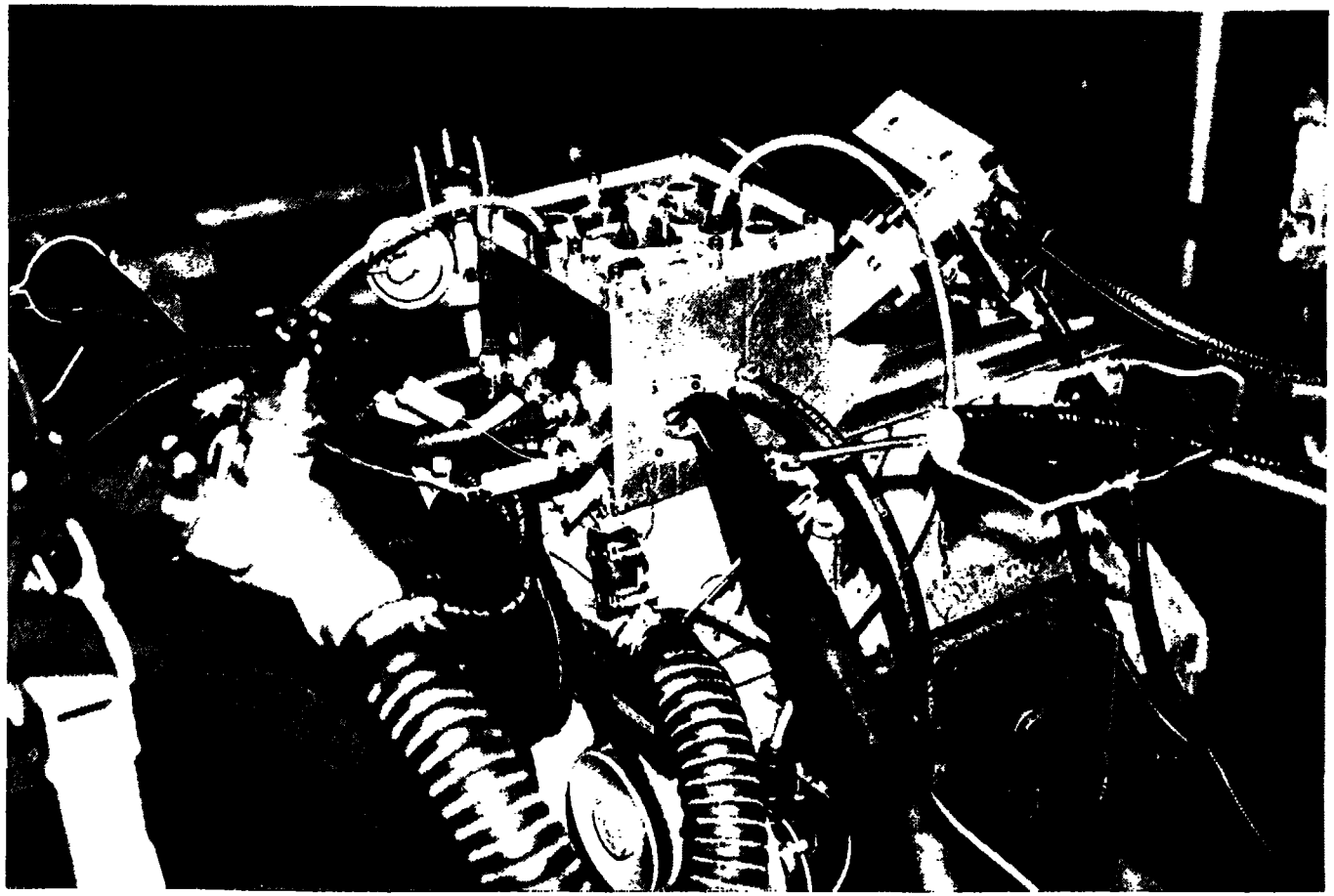

Photo 6 - Fully assembled engine

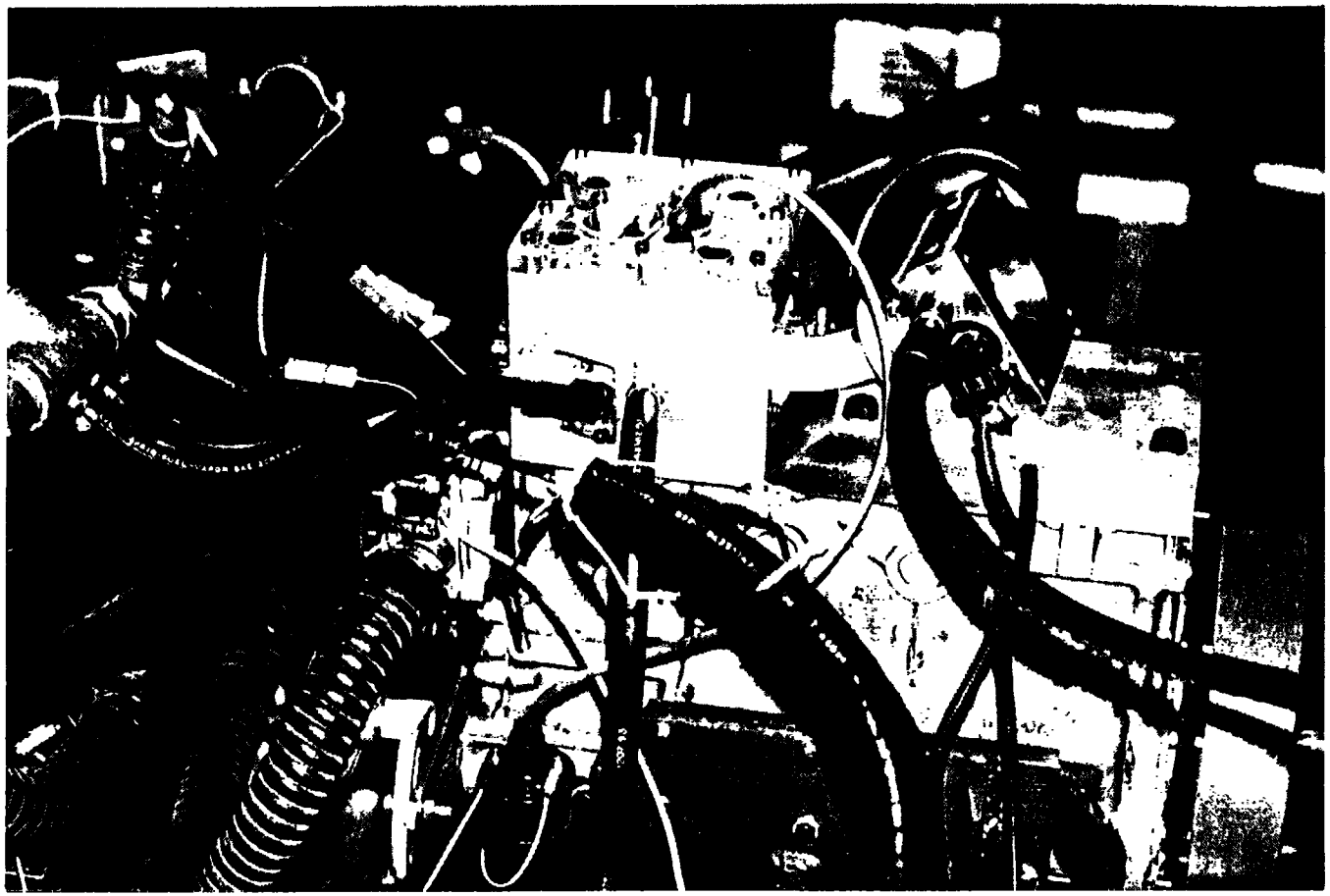

Photo 7 - Fully assembled engine

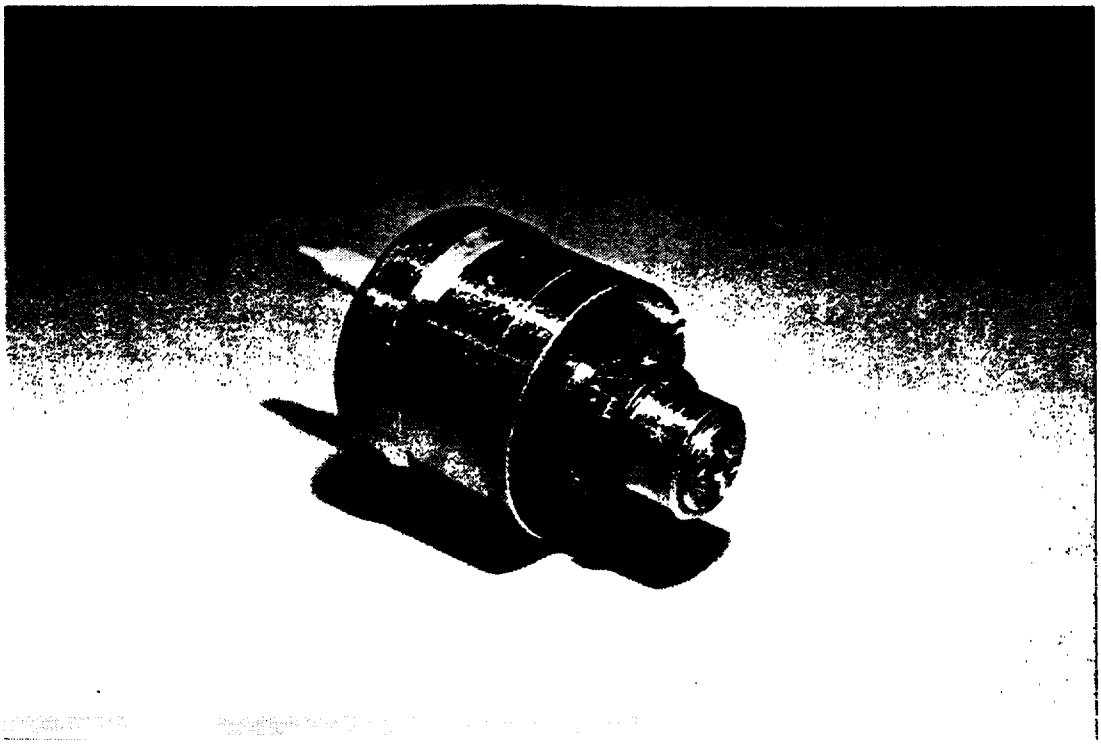

Photo 8 - Siemens injector

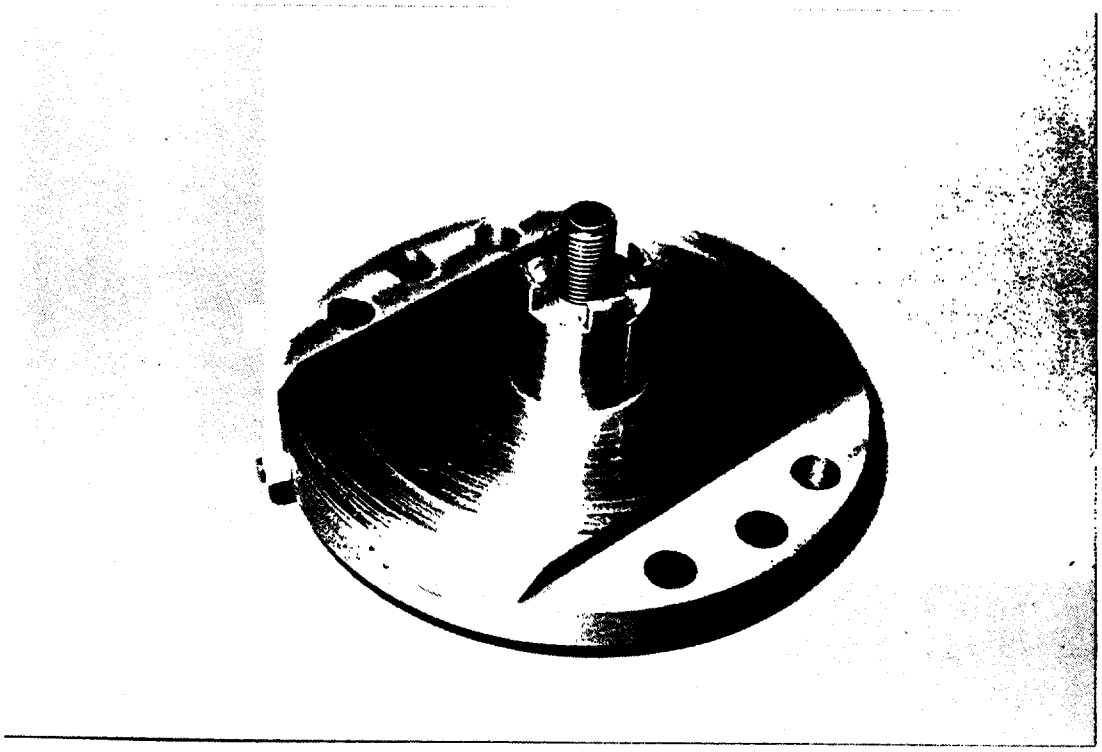

Photo 9 - Cam position disk with magnet installed for hall sensor

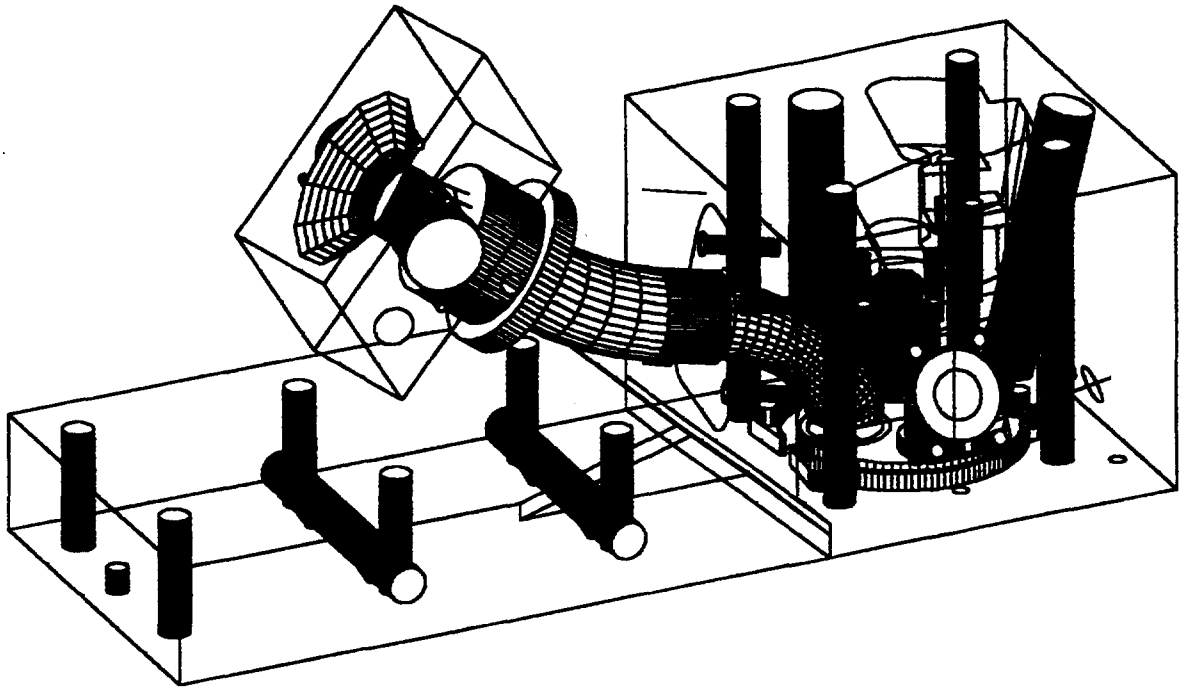

Figure 7 - CAD drawing of engine with induction system

port. The insulating tubing was used for all the unthrottled testing . No liner was used for the throttled data points.

The injector location was chosen to mitigate the negative effects of injector leakage. The inlet system was designed to deliver pure air during the beginning of the intake stroke. Should the hydrogen injector leak, it was important to place it far enough from the intake valve such that hydrogen did not collect near the intake valve during the 480° of crankshaft rotation when the intake valve was closed. Placing the injectors at the beginning of the intake manifold reduced the system's sensitivity to injector leakage. The diffusion rate of hydrogen in air is much too slow to allow significant penetration of the hydrogen into the intake port during the intake valve closed time.

Oil Control

Oil control is important in Pre-IVC (Intake Valve Closing) hydrogen-fueled engines. Excess oil consumption produces two types of problems during hydrogen operation. During light load operation, excess oil in liquid form collects on top of the piston. As long as temperatures remain low, the oil can remain in the liquid state. Transition to high-load operation causes vaporization of the oil and pre-ignition due to the oil vapor. If the oil leaves substantial deposits after vaporization, the deposits themselves can cause surface ignition.

The vaporization temperature of 10 different oils was measured prior to choosing an engine oil for this work. The testing was done by placing the oil in a depression cut in an aluminum block. The aluminum block was instrumented with thermocouples and heated from the bottom (see

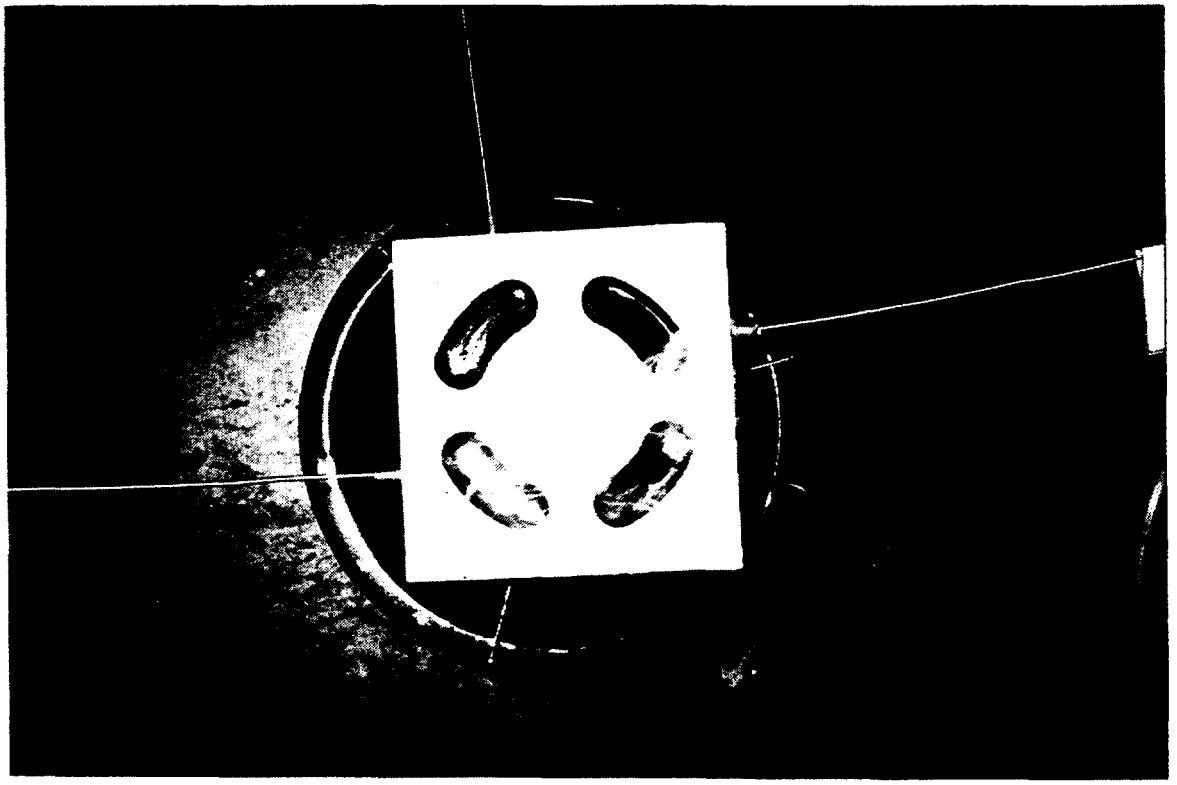

Photo 10 - Aluminum block used for oil comparison tests

Photo 10). The temperature at which vaporization took place was recorded and is shown in Table 2. AmsOil 10w-30 was chosen as the engine oil.

Table 2

AmsOil 10w-30	383 °F
Synthoil 10w-30	349 °F
Chevron HDAX 30w (low ash)	358 °F
Torco 5w-30	353 °F
Redline 10w-30	350 °F
Havoline 5w-30	337 °F
Havoline 10w-40	357 °F
Mobil 1 10w-30	383 °F
Castrol 30w	378 °F
Valvoline 30w	371 °F

Oil enters the combustion chamber at two locations: between the valve stem and valve guide, and between the piston and cylinder wall. The measures taken to prevent oil passage past these locations for gasoline-fueled engines are not in general sufficient for hydrogen-fueled engines.

Valve-stem seals limit oil passage between the valve stem and valve guide. A variety of seals were tested for use in this work. Valve-stem seal availability eventually dictated intake valve

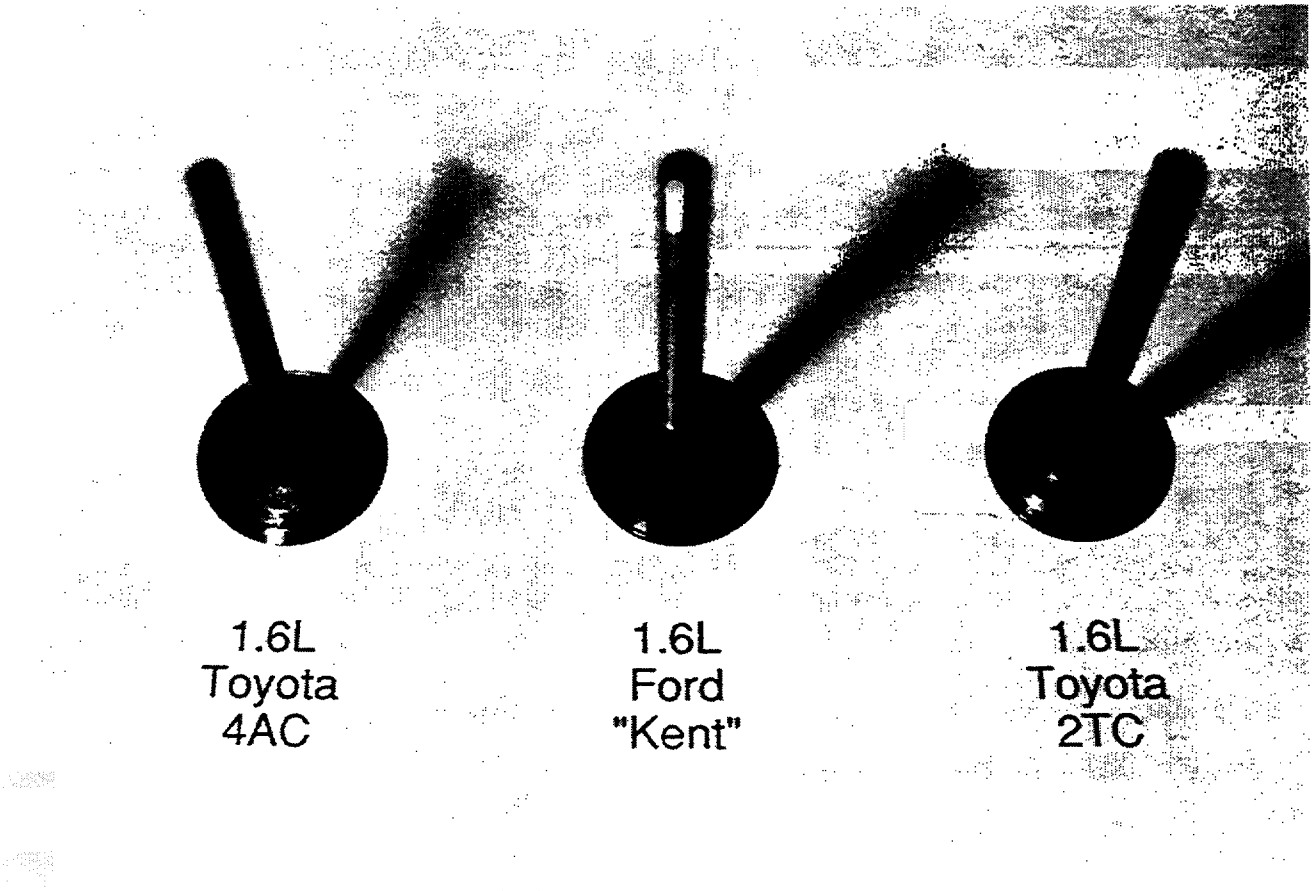

Photo 11 - Three intake valve types used during cylinder head development

selection. The original design of the cylinder used an intake valve from the 1.6 liter single overhead cam (SOHC) Toyota four-cylinder engine (4AC) (Part no. 137-11-15010) (Photo 11). The valve had a 1.42 inch head diameter and a 0.276 inch stem diameter. Difficulty in obtaining a proper valve spring/valve retainer match required a change to the intake valve from the Ford 1.6 liter "Kent" four-cylinder engine (TRW part no. V2914) (Photo 11). That valve had a 1.42 inch head diameter and a 0.309 inch stem diameter. The valve was used with the standard Ford valve guide and seal. It was not possible to obtain adequate oil control with the standard parts as designed for gasoline operation. Inspection (Photo 12) showed the valve stem had been polished preferentially on one side. This was caused by the valve-stem seal mounting location on the valve guide not being concentric with the valve stem by 0.005 inches. The valve guide was then machined to provide a concentric mounting location for the valve-stem seal.

Previous experience had shown that very good oil control could be obtained with the seven-groove, labyrinth-type valve-stem seals used on the 2.0 liter Chevrolet four-cylinder engine (Photo 13). Both five-groove and seven-groove seals were used interchangeably for gasoline operation in the Chevrolet engine, but the seven-groove seals yielded superior oil control. These valve-stem seals required an 8 mm valve stem, so a third valve for the prototype engine was made from the intake valve for a 1.6 liter 2TC Toyota four-cylinder engine (Photo 11). The intake-valve head diameter was reduced from 1.61 inches to 1.42 inches, and Toyota valve stem

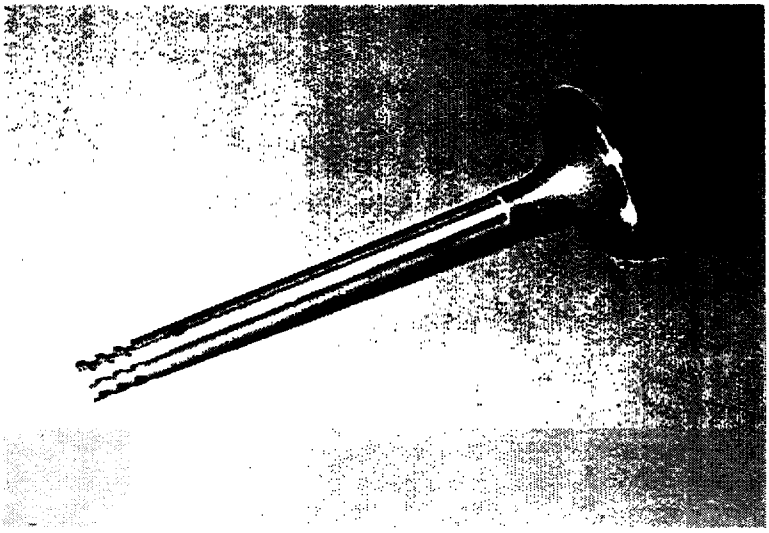

Photo 12 - Valve stem showing preferential polishing

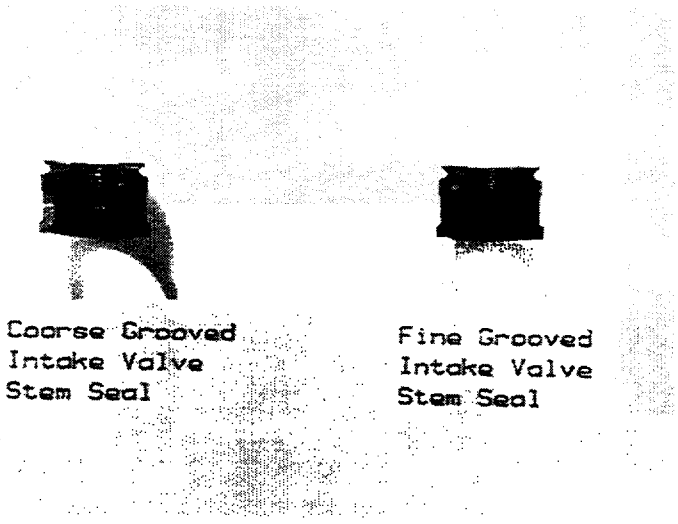

Photo 13 - Valve stem seals

locks were used together with the Ford valve retainer and spring. This combination, together with the seven-groove Chevrolet valve-stem seal, solved the oil control problems. Valve-stem O-ring seals from a 5.7 liter Chevrolet V-8 were used in the valve retainer to prevent oil passage between the valve stem and the retainer.

The final configuration to seal the exhaust valve stem was to use hand fitted (spring tension adjusted by hand) teflon 11/32 inch diameter seals.

Piston rings limit oil passage between the piston and cylinder wall. Previous work had shown that the standard Toyota ring package provided adequate oil control most of the time but not always. The most recent work using the Toyota ring package required 10 hours of break-in to produce a dry piston (free of liquid oil) during light-load operation. Having been told by ring manufacturers that this time could be reduced to 4 hours, and having seen dry operation in as little as 0.5 hours, various ring packages were tested. There are several types of rings, and the surface of the ring that touches the cylinder bore can be shaped in various ways (see Figure 8). The standard Toyota ring package consists of a chrome moly, barrel-face top ring, a cast-iron straight-cut second ring, and a 0.1064 inch radially thick pair of oil control rings. Deves Corporation rings were tested. The Deves ring package contained a cast-iron, straight-cut-face top ring, a cast-iron oil trap second ring, and a 0.1400 inch radially thick pair of oil control rings. The package took longer than the Toyota package to seat properly. Sealed Power rings were tested. The Sealed Power ring package consisted of a cast-iron 1°-tapered-face top ring, a cast-iron 1°-tapered-face second ring, and a 0.095 radially thick pair of oil control rings. This package seated rapidly and gave good oil control, showing a dry piston after only 0.5 hours of operation. This can be seen in Photo 14 which shows the cylinder bore after one-half-hour of break-in. The cylinder bore above the compression ring is dry enough to have oxidized. For this piston ring combination oil control was very good but piston scuffing occurred during high-load operation (Photo 15). To solve the scuffing problem, on the side of the piston loaded during the power stroke, the piston skirt was chamfered at the bottom. No further scuffing occurred. During the final operation of the engine, a standard Toyota top ring was substituted for the Sealed Power top ring because seating was very rapid, and the chrome moly barrel face was easier to "read" during inspections.

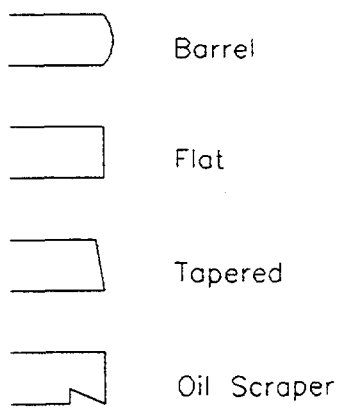

Figure 10 - Piston ring design types

The piston chosen is shown in Photo 16. Piston design was dominated by the desire to maintain a reasonably large skirt thickness. This was needed to improve heat transfer from the piston head/ring land area to the piston skirt. Cast pistons were chosen to satisfy that requirement. Scuffing was experienced during testing of the first piston, but was alleviated by modifying the piston-skirt geometry of the second piston. The crankcase was vented through a production Ford check valve.

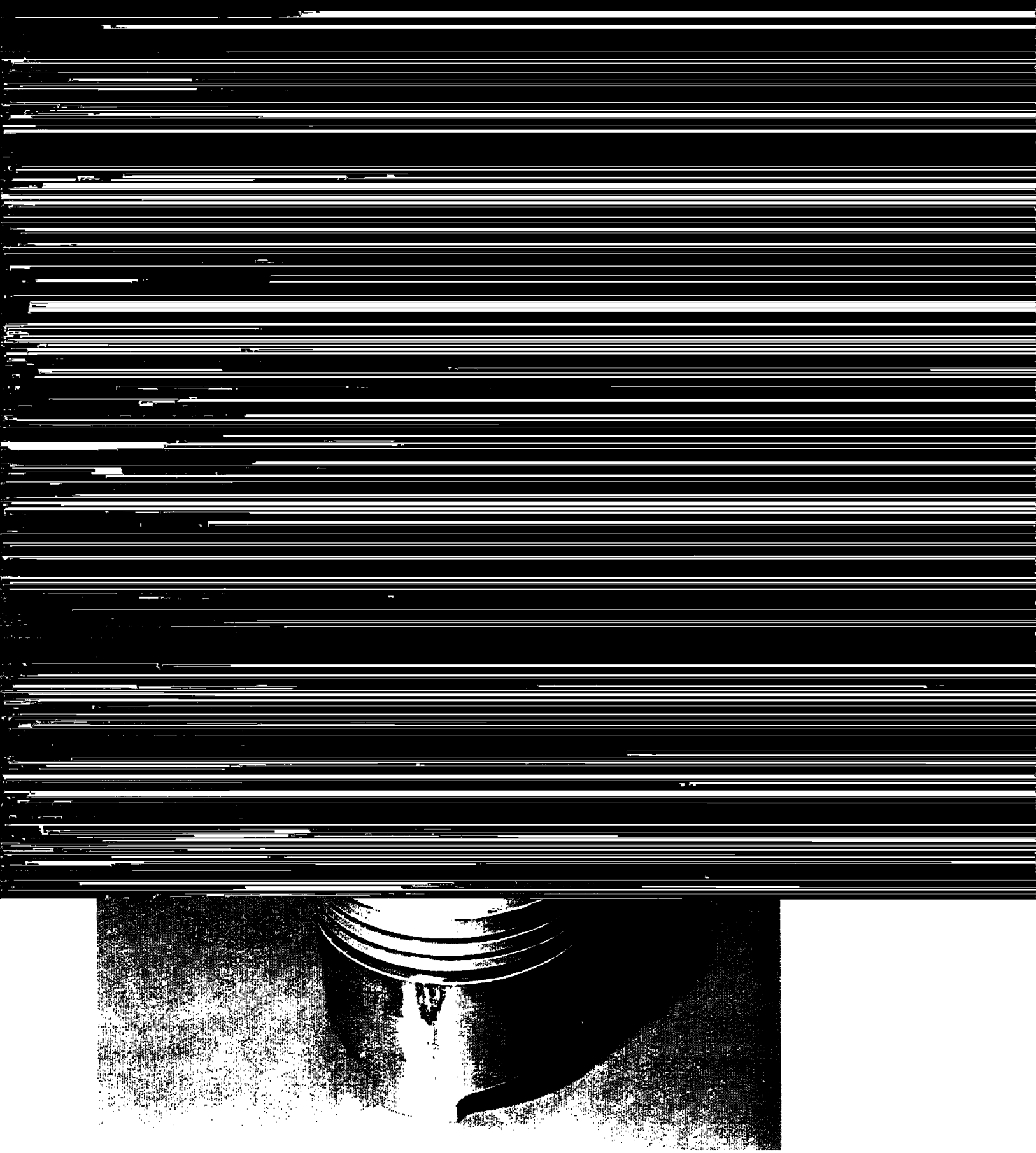

Photo 15 - Initial piston design showing scuff marks from high load operation

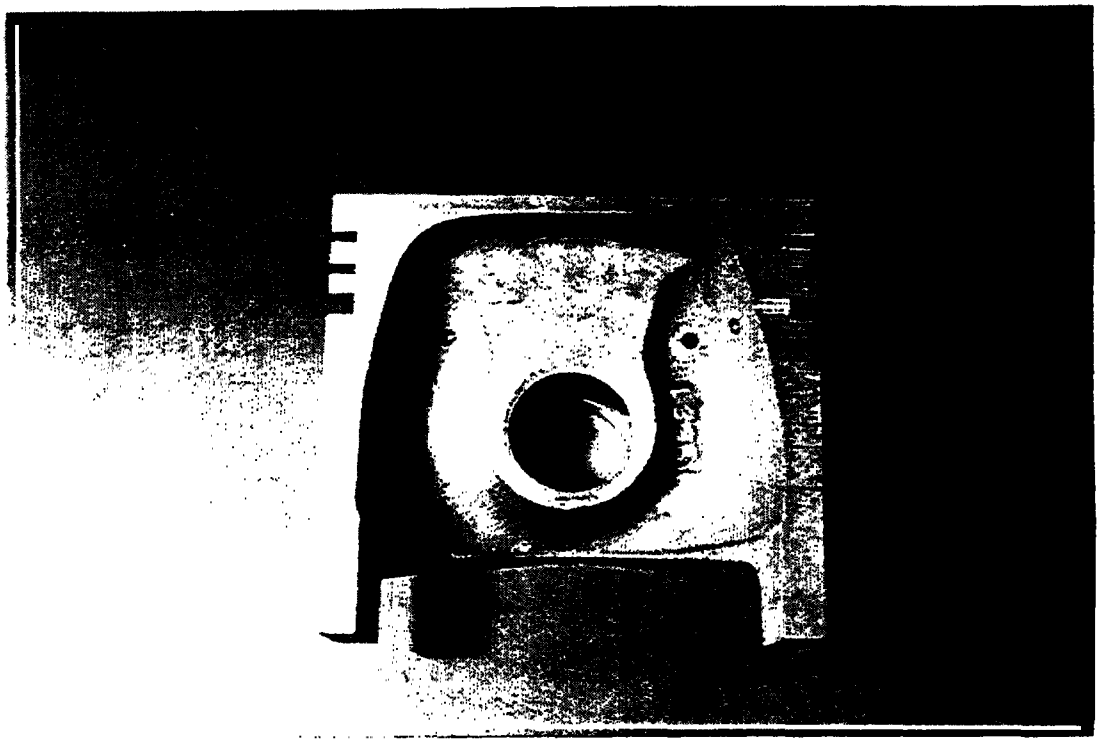

Photo 16 - Cut away view of piston design

Repeatability of Data

This project included the conversion of a four-cylinder engine to single-cylinder operation. This modification would have quadrupled the frictional mean effective pressure (FMEP) (friction per displacement); however the removal of three of the pistons, a portion of the camshaft, and the valve train from the deactivated cylinders mitigated some of the increase in FMEP. All of the original main bearings remained in the engine as well as the original oil pump and water pump, so frictional losses in the prototype engine were still very high.

The oil temperature used during testing was low (145 °F), and this also increased the frictional losses. The engine has separate cooling passages for axial heat transfer from the combustion chamber and exhaust ports and radial heat transfer from the combustion chamber and cylinder block. That allowed relatively independent control of the cylinder-head temperature and cylinder-block temperature. The oil temperature was almost strictly a function of cylinder-block temperature. The three rear cylinders had their pistons and connecting rods replaced with counterweights. The counterweights allow oil to pass out of the sides of the connecting rod bearings in the same manner as the original connecting rod. This oil is thrown onto the inside surfaces of the cylinder-block, which acted as a heat exchanger, bringing the oil temperature to the cylinder-block temperature. Because the cylinder-block was heated by the water coolant in the rear three cylinders, the engine oil temperature was always within 4° F of the water inlet temperature during steady-state operation. The FMEP due to the oil pump and bearings was a strong function of oil temperature. To determine how critical oil temperature was, tests were run with the prototype engine fueled with methane. The engine was run at 1800 RPM and 75.1 psi

brake mean effective pressure (BMEP) with constant airflow and fuel flow. The engine test results are shown in the table below:

Oil Temperature Tests

RPM	1800	1800
Oil Temperature	135 °F	155 °F
Oil Pressure	36.5 psi	29.6 psi
BMEP	75.1 psi	79.9 psi

The changes in BMEP for the two operating points is a direct result of the change in friction in the engine. Both operating points had virtually identical heat losses because the cylinder head temperature measured at the exhaust valve seats was the same for both points. The coolant flow to the cylinder head did not have to be adjusted to maintain constant cylinder-head temperature. The flow of coolant water from the cylinder block to the radial heat transfer passages in the cylinder block was minimized.

The tests indicated that the oil temperature had to be held constant in order to obtain repeatable data. The oil temperature was held at 145 °F ±2.0 °F for all data taken on hydrogen.

Method of FMEP Determination for Prototype Engine

For this research effort the FMEP at wide open throttle (WOT) was assumed to be a function of RPM only. This assumption applies particularly well to a four-cylinder engine converted to single-cylinder operation. A large portion of the internal friction in an engine converted to single-cylinder operation is caused by unloaded crankshaft bearings, the oil pump, and the water pump. These friction-producing engine parts are not affected by cylinder pressure and, consequently, do not change with engine load.

An example of how FMEP changes with load is seen in Ball, 1986. The FMEP for a 1.6 liter four-cylinder engine at 1800 RPM is given at two load conditions: 29.4 psi BMEP and 88.2 psi BMEP. The total FMEP was 5.4 psi higher at 29.4 psi BMEP than at 88.2 psi BMEP. The reason the lighter load shows a much higher FMEP than the high-load condition is because reduction in load created large pumping losses. If a comparison is made of the piston-crank assembly friction losses at low and high load, the FMEP is 0.5 psi higher at the higher load. The pumping losses do not change appreciably with load in an unthrottled engine. The dedicated hydrogen engine operated unthrottled. The changes in FMEP averaged 0.5 psi over a much larger change in load than those used in this research activity.

As noted previously, FMEP was a very strong function of oil temperature, so all measurements were made at 145 °F oil temperature. The FMEP was measured while operating the engine on one spark plug and using the other spark plug location for a pressure transducer. The FMEP was measured at 1000, 1800, 2830, and 4000 RPM, with dried exhaust oxygen content equal to 12%. Cylinder pressure diagrams were recorded using a Kistler 640-601B pressure transducer with a Kistler 5002D charge amplifier and Nicolet 2090-III digital oscilloscope. Engine load was

measured using the electrodynamometer. An aluminum disk with indexing holes drilled every two degrees was mounted on the crankshaft to directly trigger the digital oscilloscope, using a phototransistor, to take data at known crankshaft positions. The camshaft hall sensor signal was used to start the recording of cylinder pressure data 21° BBDC on the intake stroke to ease post-processing of the results. A counter, tracking the crankshaft position, was used to zero the charge amplifier during the exhaust stroke of every cycle. The cylinder pressure traces thus recorded were then integrated, with respect to cylinder volume, off line to calculate indicated mean effective pressure (IMEP). A common cause of error in IMEP calculation using this method is error in the crankshaft position measurement. Taking pressure-time data and assuming constant RPM to calculate crankshaft position does not yield accurate results because RPM varies too much during the cycle[1]. Indexing on the crankshaft disk eliminated that problem, and a separate hole on the disk at top dead center was used to produce a marking signal on the second channel of the oscilloscope to verify that the data was in register. The measured BMEP values were subtracted from the IMEP values calculated in this manner to compute FMEP.

The change in FMEP due to pumping losses was measured by motoring the engine at a specific RPM and varying the throttle position. Measurements of the change in FMEP were made with the throttle position producing specific desired volumetric efficiencies.

Experimental Technique

1. Measure atmospheric pressure.
2. Measure humidity.
3. Set hydrogen delivery pressure at 45 psi.
4. Position the cam mounted injection timing disk at the desired injection timing.
5. Set injector duration desired.
6. Start engine and run for 60 minutes on liquified petroleum gas (LPG) or natural gas to warm up to 145 °F oil temperature and 225 °F seat temperature.
7. Switch to hydrogen fuel.
8. Increase hydrogen pressure to slightly rich operation (measured O_2 low).
8. Reduce injection duration to match desired fuel-air mixture.
9. Adjust spark advance, water flow in cylinder head, water flow in cylinder block, dynamometer, and fuel flow rate until 225 °F exhaust seat temperature and 145 °F oil temperature is reached with best efficiency spark advance (BESA) and the desired measured oxygen in the exhaust.

Measure and record

Exhaust seat temperature (225 °F)
Oil temperature (145 °F)
Air flow
Oxygen content in the exhaust (condensed exhaust)
NOx

---

[1]This can be alleviated to some extent by the use of a high moment of inertia flywheel.

RPM
Load
Fuel flow

EQUIPMENT USED DURING THIS RESEARCH ACTIVITY

Exhaust Emission Measurements

A Beckman Model OM-11 Polarographic Oxygen Analyzer was used to measure O_2 concentration in the exhaust. The exhaust sample was dried by cooling in a condenser. Measurements were corrected for the loss in sample volume caused by drying.

Fuel and Air Flowrate Measurements

Because the confidence level of measured brake-specific fuel consumption and fuel-air equivalence ratio are critically dependent upon the accuracy of fuel flowrate and air flowrate measurements, a survey was made of the available flowrate measuring devices. With the help of Dr. David W. Baker of the National Bureau of Standards, Fluid Mechanics Department, high accuracy rotameters were selected to measure fuel flowrate and air flowrate as described below.

Fuel Flow Meters

Among the criteria for the flowrate meter selection are: high precision, low bias error, ease of maintenance, low fuel pressure requirements, and reasonable cost. It is desirable to have more than one meter to bridge the entire range of fuel flowrate (140:1). With multiple meters, the ranges can be overlapped, affording the opportunity to conduct pretest calibration checks in the overlap regions. An additional criteria to be considered when choosing a particular flowmeter type is resolution; it varies with the length, dynamic range, and type of tube taper. For example, Co Instrument gives a resolution of ±1% for its logarithmic tube 120 model, which has a large dynamic range (13:1), and ±0.5% for its logarithmic tube 129 model, which has a small dynamic range (5:1).

Based on the above considerations, a high-precision rotameter with a potential precision of ±0.2% of reading and an estimated bias error of ±0.5% of reading was selected, along with a high-accuracy mercury manometer and a certified standard calibrated thermocouple to measure the fuel flowrate. The meter was manufactured by Co Instrument (Model 129-287 Range) and is composed of three logarithmic tubes, each having a resolution of about ±0.5% of reading.

Calibration for standard application, high-accuracy flow meters is conducted by using air as a flow medium and then modifying the calibration curves by using the appropriate standard correction factors for the fluid to be metered during the tests. This procedure is expected to result in accuracies of ±1% for high-precision meters. To improve the accuracy to ±0.5%, the Colorado Experimental Engineering Station, Inc. (CEDES), Boulder, Colorado, calibrated each of the logarithmic tubes used in the present study with hydrogen as the calibration fluid.

Because the rotameter is a volumetric flowmeter, the pressure and temperature of the metered fluid must be measured to ascertain mass flowrates. Errors in these measurements reduce total accuracy. The estimated uncertainty for the fuel mass-flowrate measurement was approximately ±0.8%, found by calculating the root mean square of the following components (at full scale)

Manufacturer meter resolution claim	±0.5%
Calibration error	±0.5%
Temperature uncertainty error (±0.5°F)	±0.2%
Barometric Pressure uncertainty	±0.07%
Hg Manometer uncertainty	±0.25%
Estimated uncertainty (95% confidence)	±0.8%

Air Flow Meters

Air flow measurements were made using a laminar flow element that had a certified accuracy of ±0.65% of reading, and a high-precision inclined manometer for pressure drop measurement that had an certified accuracy of ±0.25% of reading. The following instruments were selected.

Meriam 50 MC2-2F Laminar Flow Element
Meriam 40H35, 50" Scale Manometer

As with the fuel-flow measurements, it was necessary to ascertain the density of the air by measuring air pressure and temperature. In addition, it was necessary to determine the humidity of the air. The estimated uncertainty for the air mass-flowrate was approximately ±0.8%, found by calculating the root mean square of the following components at full scale.

Calibration of Laminar Flow Element error	±0.65%
Calibration Table Resolution	±0.25%
Resolution of 50" Scale Manometer	±0.25%
Temperature uncertainty error (±0.5°F)	±0.2%
Barometric Pressure uncertainty	±0.07%
Hg Manometer uncertainty	±0.25%
Estimated uncertainty (95% confidence)	±0.8%

Fuel-Delivery Systems

The hydrogen was stored in standard welding-type tanks. During the experiments, the temperature and pressure in the tanks decreased as the gas was consumed. To minimize the temperature decrease, a fuel-delivery system consisting of two sets of four tanks connected in parallel was used. During the tests, fuel was emptied simultaneously from all four tanks of one set. Upon depletion of the fuel in one set, the other set could be turned on allowing for continuous operation without shut-down. In addition to the simultaneous use of four tanks, the fuel was passed through a coil of tubing immersed in a constant-temperature bath to aid in maintaining a constant temperature at the flowmeter. There was also a 70-cu-in. surge tank installed to damp

pressure pulses. A two-stage pressure regulator downstream of the individual tank regulators was used to give precise control over the pressure level at the fuel flow meters. This fuel pressure was measured with a precision mercury manometer having an accuracy of ±0.07% of reading.

In-Cylinder Pressure-Time Diagrams

The following components were used to measure in-cylinder pressure-time diagrams during FMEP determination.

1. Kistler piezoelectric pressure transducer part# 601B2
2. Adapter to install transducer in spark plug location
3. Kistler charge amplifier part# 5004D
4. A Nicolet 2090 Digital Oscilloscope

The cylinder-pressure versus crank-angle data were gathered with a piezoelectric pressure transducer installed in one of the spark plug locations.

The transducer was calibrated in combination with the 5004 charge amplifier using two high-precision pressure gauges as references. Valves were arranged to apply a step change in pressure at the transducer. The calibration of the transducer-amplifier pair corresponded to the factory calibration of the transducer within ±0.7%. Also, the charge amplifier included an external zeroing feature that was controlled by hardware that zeroed the amplifier during the exhaust stroke of each cycle. DC offset in the amplifiers (error in output voltage with zero input voltage) could be checked, before or during testing, with the oscilloscope.

The amplifier signal was digitized with the digital oscilloscope. A 12-in. aluminum disk with holes around the circumference spaced at 2° intervals was used in conjunction with two phototransistors to determine crankshaft position. Top dead center (TDC) was located by noting the crank shaft position on either side of TDC when the piston had descended 1.2 inches into the bore. At this piston position, 1° crankshaft rotation produces 0.040 inches piston movement. The piston had no piston pin offset. The crankshaft was then positioned at the point between these two locations. The phototransistor sensors were aligned to the disk with two pins that fit through the sensor holes and through the TDC holes in the 12-in. disk. The sensor housing was then tightened to its mount. The hardware received pulses from this crankshaft position sensor system and computed crankshaft position using a counter. The hardware strobed the digital oscilloscope to take pressure data as a function of crankshaft position rather than versus time.

Although the spark plug adapter served to protect the transducers from peak combustion temperatures, the transducer was coated with a silicone protective coating (General Electric RTV 116 Silicone Sealant). This precaution was taken because of concern for the small quench distance of a hydrogen flame.

Cylinder pressure and crank angle were measured over 120 cycles to yield time-averaged pressure versus crank angle traces for the IMEP calculations.

Measurement of Equivalence Ratio

The measurement of equivalence ratio was done by two independent methods during this research project. The first method involved measuring oxygen content in the dried exhaust and performing a chemical balance to determine the equivalence ratio. This method resulted in a measurement of equivalence ratio in which a 0.1% change in oxygen content in the exhaust produced a 1% change in calculated equivalence ratio.

The second method involved measuring fuel flow and air flow with flow meters and computing the equivalence ratio from those measurements.

The first method was used for data with an equivalence ratio greater than 0.5. The second method was used for data with an equivalence ratio less than 0.5. During operation at equivalence ratios less than 0.5, the oxygen content in the exhaust was used as a guide when changing the engine operating point, and the fuel and air flow measurements were used to verify the equivalence ratio once the operating point had been reached.

CONCLUSIONS

The following features were included in the design of this prototype hydrogen-fueled engine in an effort to eliminate abnormal combustion in a hydrogen-fueled engine.

1. Timed induction to allow air with little or no hydrogen to enter the combustion chamber during the early part of the intake stroke.

2. Inertially tuned exhaust system to reduce the quantity of residuals trapped in the cylinder after the exhaust stroke.

3. Design of the coolant passages and the use of once-through city water to reduce cylinder head temperatures.

4. Reduced coolant temperatures to reduce oil and cylinder-block temperatures.

5. Two sodium-cooled exhaust valves to reduce the exhaust valve surface temperatures.

6. Side-gap spark plugs to reduce spark plug surface temperatures.

7. Thick piston-skirt design to reduce piston surface temperatures.

8. Minimized top compression ring gap to reduce piston ring crevice flow.

The modifications allowed the engine to be operated at WOT stoichiometric equivalence ratios in the laboratory during data taking. This is not meant to imply that the engine could be used on a daily basis without developing abnormal combustion.

Figures 9 and 10 show measured pressure versus crank angle data for WOT, equivalence ratio 1.06. These two figures were chosen because they clearly show the cycle-to-cycle variation in ignition lag. Ignition lag varied from 2° to 4°.

Figures 11 and 12 are indicated performance maps for the engine. These were generated by using the 17 data points from Appendix A. The maps are useful for viewing trends and approximate values, but their accuracy is limited by the number of points used to generate them.

Acknowledgement

The authors would like to acknowledge the support and extraordinary patience of NREL and DOE. The additional time allowed investigation of timed fuel injection, not originally included in the work effort.

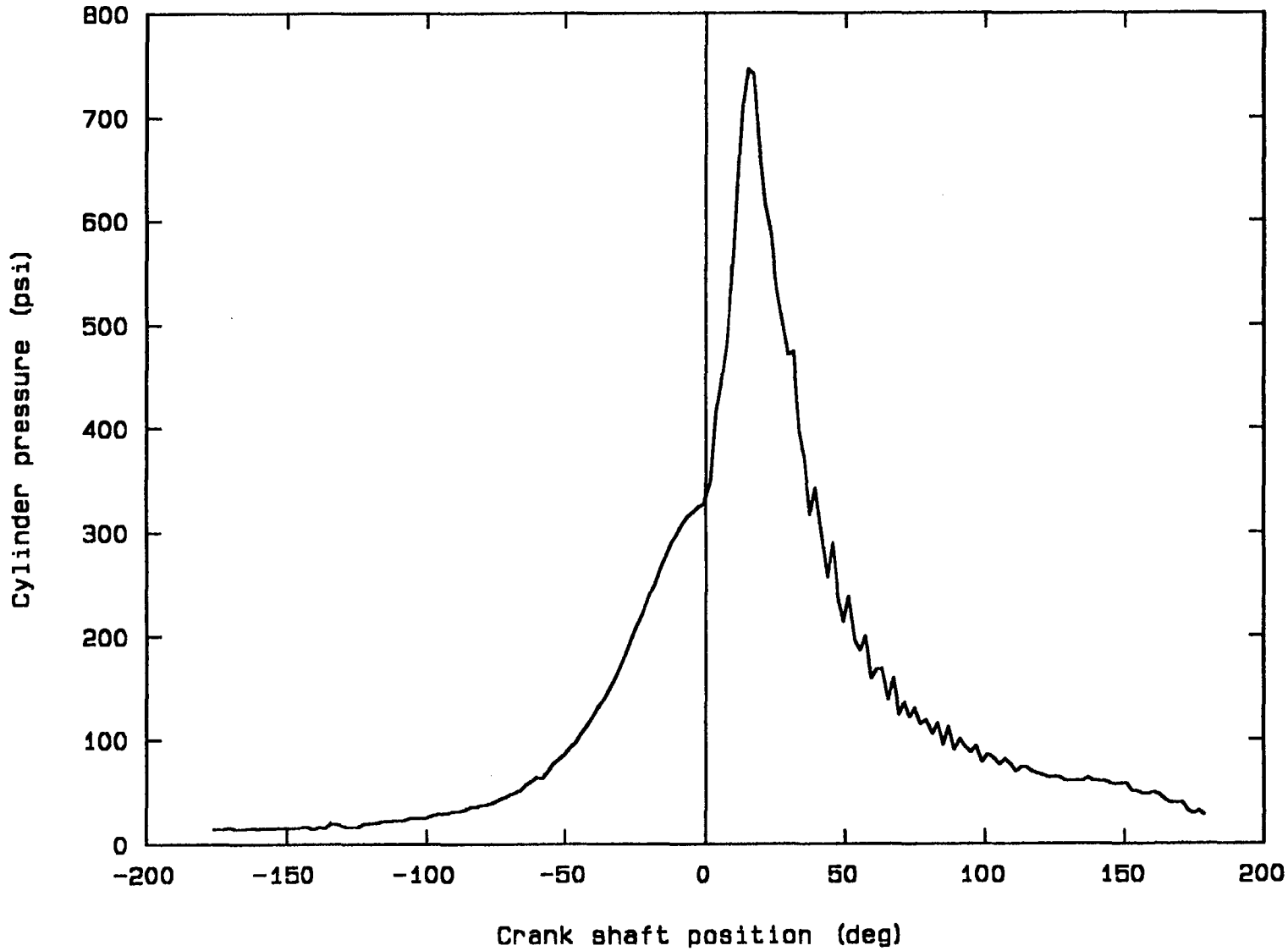

Figure 9 - Pressure versus crank angle, SA - 2° BTDC, WOT, equivalence ratio - 1.06

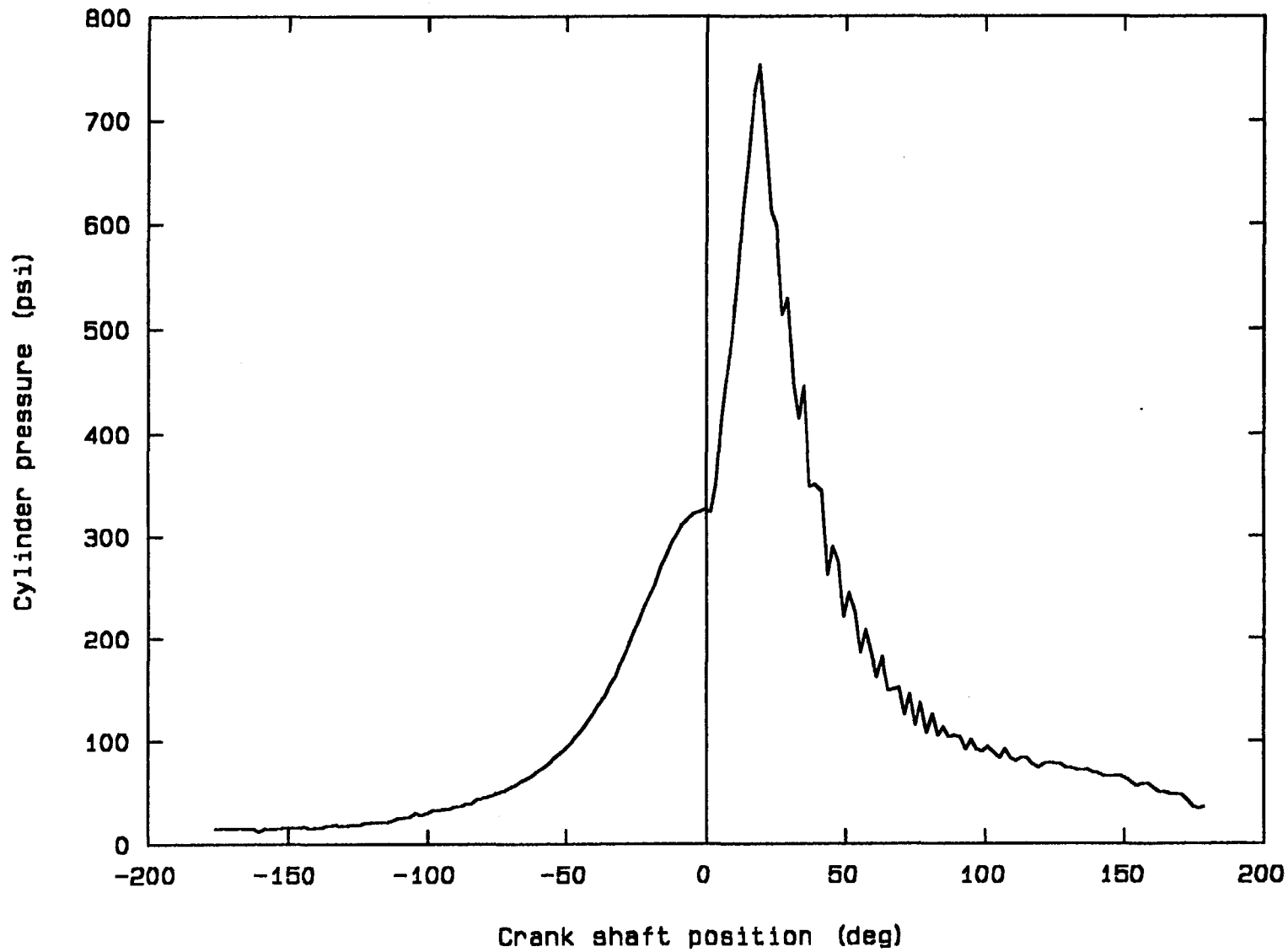

Figure 10 - Pressure versus crank angle, SA - 2° BTDC, WOT, equivalence ratio - 1.06

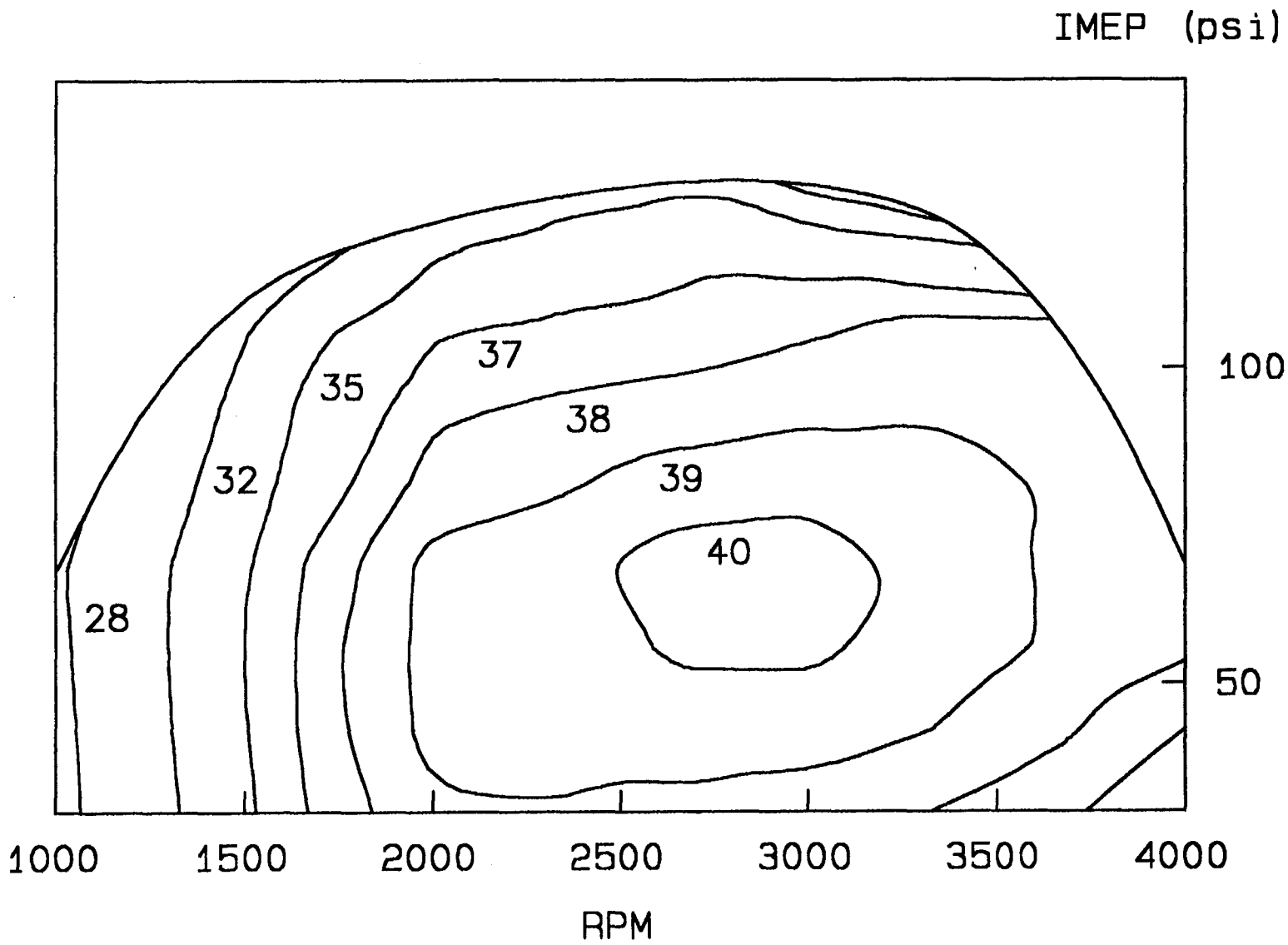

Figure 11 - Engine indicated thermal efficiency performance map

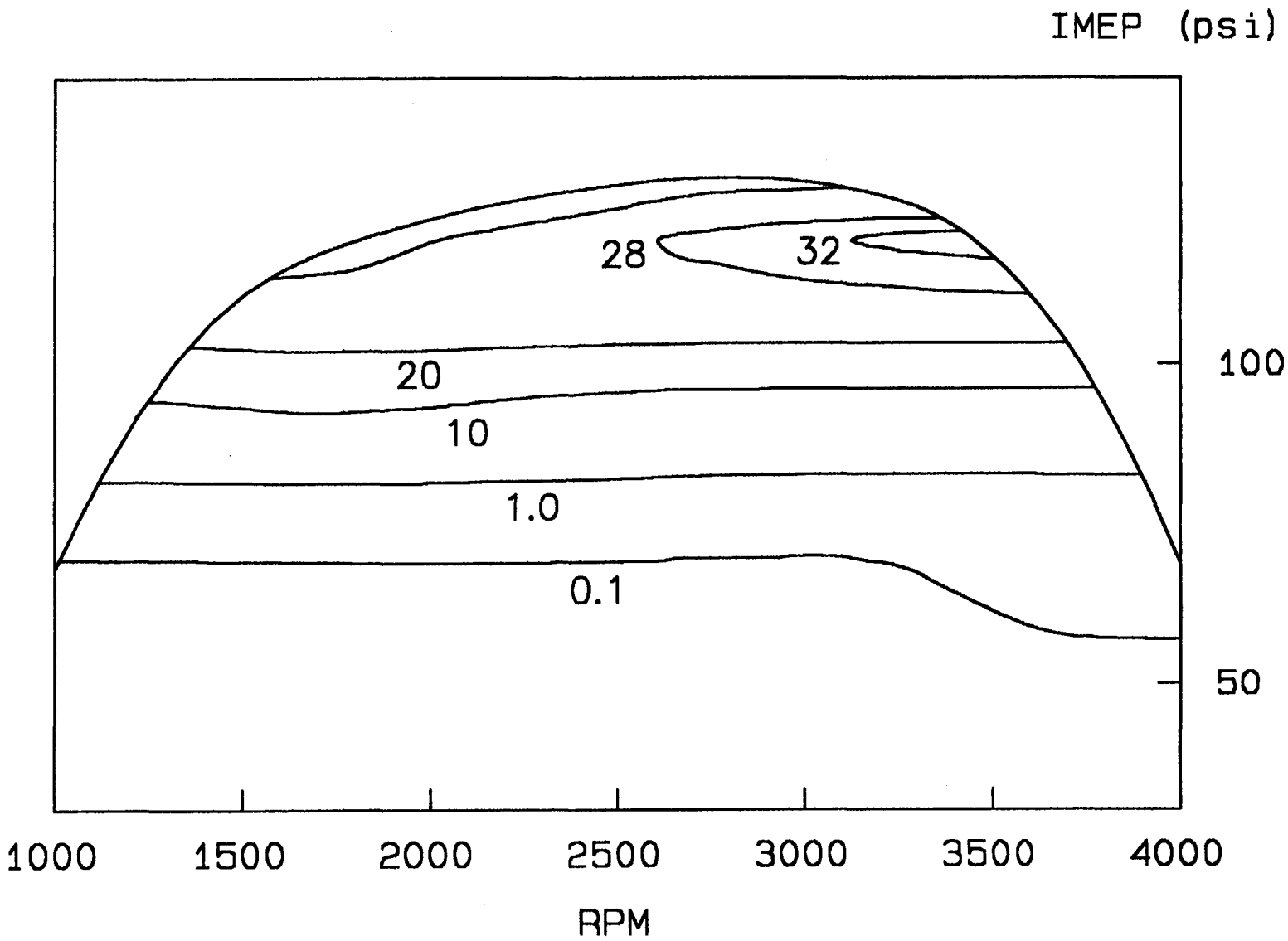

Figure 12 - Engine indicated specific NO_x production (gm/hp-hr) performance map

Appendix A

The following are tables of measured data from the engine :

RPM	1800	3500	1000	1800	2830	3500	4000
Volumetric Efficiency (%)	49.9	62.9	79.0	84.6	87.9	88.4	74.3
Equivalence Ratio	0.4	0.4	0.4	0.4	0.4	0.4	0.4
BMEP (psi)	5.7	-2.4	37.1	36.3	30.7	21.0	4.8
FMEP (psi)	34.1	53.1	21.1	30.5	42.7	50.3	56.5
IMEP (psi)	39.8	50.7	58.2	66.8	73.4	71.3	61.3
ITE (%)	38.6	39.1	36.0	38.6	40.7	39.2	40.2
Spark Advance (°BTDC)	32	34	23	27	31	33	35
NO_x (ppm)	5.7	11.5	7.4	7.9	10.2	14	18
NO (ppm)	4.4	8.8	5.1	6.0	8.4	-	-

RPM	1000	1800	2830	3500	4000
Volumetric Efficiency (%)	79.2	84.9	88.2	88.6	74.1
Equivalence Ratio	0.5	0.5	0.5	0.5	0.5
BMEP (psi)	46.8	48.4	42.8	35.5	12.1
FMEP (psi)	21.1	30.5	42.7	50.6	56.5
IMEP (psi)	67.9	78.9	85.5	86.1	68.6
ITE (%)	34.8	37.7	39.3	39.2	37.3
Spark Advance (°BTDC)	15	17	20	22	25
NO_x (ppm)	45	71	90	120	175
NO (ppm)	41	64	88	-	-

RPM	1800	2830	3500	1800	2830
Volumetric Efficiency (%)	83.7	87.3	88.0	83.1	86.5
Equivalence Ratio	0.8	0.8	0.8	1.06	1.06
BMEP (psi)	77.5	72.7	66.2	88.6	86.4
FMEP (psi)	30.5	42.7	50.6	30.5	42.7
IMEP (psi)	108.0	115.4	116.8	119.3	129.1
ITE (%)	35.9	36.8	36.9	32.6	33.9
Spark Advance (°BTDC)	5	5	6	2	3
NO_x (ppm)	5200	6800	7400	4100	4400
NO (ppm)	-	-	-	-	-

REPORT DOCUMENTATION PAGE

Form Approved
OMB NO. 0704-0188

1. AGENCY USE ONLY (Leave blank)	2. REPORT DATE	3. REPORT TYPE AND DATES COVERED
	November 1995	Final Report

4. TITLE AND SUBTITLE

Elimination of Abnormal Combustion in a Hydrogen-Fueled Engine

5. FUNDING NUMBERS

(C)
(TA) FU521010

6. AUTHOR(S)

M. R. Swain and M. N. Swain

7. PERFORMING ORGANIZATION NAME(S) AND ADDRESS(ES)

University of Miami, Coral Gables, Florida; Analytical Technologies, Inc., Miami, Florida

8. PERFORMING ORGANIZATION REPORT NUMBER

DE95009277

9. SPONSORING/MONITORING AGENCY NAME(S) AND ADDRESS(ES)

National Renewable Energy Laboratory
1617 Cole Boulevard
Golden, CO 80401-3393

10. SPONSORING/MONITORING AGENCY REPORT NUMBER

NREL/TP-425-8196

11. SUPPLEMENTARY NOTES

12a. DISTRIBUTION/AVAILABILITY STATEMENT

National Technical Information Service
U.S. Department of Commerce
5285 Port Royal Road
Springfield, VA 22161

12b. DISTRIBUTION CODE

UC-1504

13. ABSTRACT (Maximum 200 words)

This report covers the design, construction, and testing of a dedicated hydrogen-fueled engine. Both part-load and full-load data were taken under laboratory conditions. The engine design included a billet aluminum single combustion chamber cylinder-head with one intake valve, two sodium coiled exhaust valves, and two spark plugs. The cylinder-head design also included drilled cooling passages. The fuel-delivery system employed two modified Siemens electrically actuated fuel injectors. The exhaust system included two separate headers, one for each exhaust port. The piston/ring combination was designed specifically for hydrogen operation.

14. SUBJECT TERMS

Hydrogen fuel; engine combustion

15. NUMBER OF PAGES

38

16. PRICE CODE

17. SECURITY CLASSIFICATION OF REPORT	18. SECURITY CLASSIFICATION OF THIS PAGE	19. SECURITY CLASSIFICATION OF ABSTRACT	20. LIMITATION OF ABSTRACT